Graz University of Technology
Institute of Applied Mechanics

Preprint Series

Preprint No 02/2014

An Efficient Galerkin Boundary Element Method for the Transient Heat Equation

Michael Messner, Martin Schanz
Institute of Applied Mechanics, Graz University of Technology
Johannes Tausch
Mathematics Department, Southern Methodist University

Published in *SIAM Journal on Scientific Computing*
37(3), A1554–A1576, 2015
DOI: 10.1137/151004422

Latest revision: January 18, 2015

Abstract

We present boundary integral representations of several initial boundary value problems related to the heat equation. A Galerkin discretization with piecewise constant functions in time and piecewise linear functions in space leads to optimal a priori error estimates provided that the meshwidth in space and time satisfy $h_t = O(h_x^2)$. Each time step involves the solution of a linear system, whose spectral condition number is independent of the refinement under the same assumption on the mesh. We show that, if the parabolic multipole method is used to apply parabolic boundary integral operators, the overall complexity of the scheme is log-linear while preserving the convergence of the Galerkin discretization method. The theoretical estimates are confirmed numerically at the end of the paper.

1 Introduction

Boundary integral equations related to the heat equation have been studied in Pogorzelski [11], Brown [3], Arnold and Nooon [1, 9] and Costabel [4]. For classically used second kind integral equations, e.g., a double layer potential approach for the Dirichlet problem and a single layer potential ansatz for the Neumann problem, the compactness of these integral operators for smooth domains, guarantees the well posedness and provides the backbone for the analysis of numerical methods. However, in the case of non smooth domains and first kind integral equations the situation is more complicated. Brown [3] gave some first results on Lipschitz domains before almost contemporaneously Arnold and Noon [1] and Costabel [4] proved the boundedness and coercivity of the thermal single layer operator. Furthermore, the latter paper showed the coercivity of the hypersingular operator and the boundedness of all thermal boundary integral operators in the appropriate anisotropic Sobolev space setting.

With these results the analysis of Galerkin methods in space and time follows the well known pattern of the elliptic theory, i.e., the Lemma of Lax-Milgram guarantees uniqueness and solvability of the corresponding operator equations and their Galerkin variational formulation. Using conforming finite-dimensional subspaces of the natural energy spaces, uniqueness and solvability translates directly to the discrete system, where Cea's Lemma provides quasi-optimality. Using the approximation property of piecewise polynomial finite-dimensional ansatz spaces, the regularity of the boundary integral operators, and assuming certain regularity of the discretization, one can derive explicit error estimates in the energy norm as well as weaker and stronger norms.

Since integral operators are non-local, discretizations lead to dense matrices and therefore, fast methods are important to handle large scale problems efficiently. This is a very well studied subject in the elliptic case, see [8], and has recently attracted considerable interest for parabolic boundary integral equations. A possible approach in this direction is to employ Fourier techniques [5]. Nevertheless, the focus here is on clustering techniques, because of their success in the elliptic case. The idea is to agglomerate source- and evaluation panels in space and time and approximate admissible interactions by a truncated series expansion. The parabolic fast multipole method was originally described in [13, 14] and successfully applied to a Galerkin scheme in [7]. In this paper we further pursue this strategy to accelerate the application of all boundary integral operators of the heat equation. We will show that the additional error introduced by the fast method can be controlled such that it is of the same order as the error of the discretization scheme.

To facilitate boundary element calculations, one has to project the given boundary data into the finite element space. Thus we extend the error analysis of [4, 9] to such an approximation. Moreover, we simplify and extend the methodology for elliptic boundary integral equations, see, e.g., [10, 12] to the parabolic case.

Finally, since integral operators of the heat equation are causal, their discretization lead to block-lower triangular matrices. Thus every time step involves the solution of a linear system, that is the discretization of an elliptic operator equation. We will derive bounds of the spectral conditioning of that system. Our main result is that if the space-time refinement scheme satisfies $h_t \lesssim h_x^2$ then the condition number remains bounded as the mesh is refined. We obtain a scheme with log-linear complexity in the number of degrees of freedom of the discretization and

conclude with numerical examples that reproduce the theoretical estimates.

2 The Heat Equation

We consider the solution of the homogeneous heat equation with homogeneous initial conditions in $\Omega \times \Upsilon$, where $\Omega \subset \mathbb{R}^3$ with piecewise Lipschitz boundary $\partial\Omega := \Gamma$ and $\Upsilon := (0,T)$ with $T \in \mathbb{R}_+$. In such a setting we state a general mixed homogeneous initial boundary value problem by

$$\Delta u(\tilde{\mathbf{x}},t) = \partial_t u(\tilde{\mathbf{x}},t)\,, \qquad (\tilde{\mathbf{x}},t) \in \Omega \times \Upsilon\,, \tag{1a}$$

$$u(\tilde{\mathbf{x}},0) = 0\,, \qquad \tilde{\mathbf{x}} \in \Omega\,, \tag{1b}$$

$$u(\mathbf{x},t) = g_D(\mathbf{x},t)\,, \qquad (\mathbf{x},t) \in \Gamma_D \times \Upsilon\,, \tag{1c}$$

$$\partial_{n_\mathbf{x}} u(\mathbf{x},t) = g_N(\mathbf{x},t)\,, \qquad (\mathbf{x},t) \in \Gamma_N \times \Upsilon\,, \tag{1d}$$

$$\partial_{n_\mathbf{x}} u(\mathbf{x},t) + \kappa(\mathbf{x},t)u(\mathbf{x},t) = g_R(\mathbf{x},t)\,, \qquad (\mathbf{x},t) \in \Gamma_R \times \Upsilon\,. \tag{1e}$$

Here Γ_D, Γ_N and Γ_R denote the parts of Γ where the Dirichlet, Neumann and Robin boundary conditions are specified. We assume that $\kappa \in L_\infty(\Gamma \times \Upsilon)$ and that $\kappa \geq 0$.

2.1 Boundary Integral Equations

It is well known that the solution of the homogeneous heat equation with homogeneous initial conditions is given by the representation formula [4, Theorem 2.20]

$$u(\tilde{\mathbf{x}},t) \;=\; \int_0^t \int_\Gamma G(\tilde{\mathbf{x}} - \mathbf{y}, t - \tau) q(\mathbf{y},\tau) \mathrm{d}s_\mathbf{y} \mathrm{d}\tau \;-\; \int_0^t \int_\Gamma \partial_{n_\mathbf{y}} G(\tilde{\mathbf{x}} - \mathbf{y}, t - \tau) u(\mathbf{y},\tau) \mathrm{d}s_\mathbf{y} \mathrm{d}\tau \;\;,$$

where $(\tilde{\mathbf{x}},t) \in \Omega \times \Upsilon$. Here $q(\mathbf{y},\tau) := \partial_{n_\mathbf{y}} u(\mathbf{y},\tau)$ is the Neumann trace of the solution on the boundary and the heat equation's fundamental solution is given by

$$G(\mathbf{x},t) = \begin{cases} (4\pi t)^{-\frac{3}{2}} \exp\left(-\frac{|\mathbf{x}|^2}{4t}\right)\,, & \mathbf{x} \in \mathbb{R}^3,\, t \geq 0 \\ 0\,, & \mathbf{x} \in \mathbb{R}^3,\, t < 0 \end{cases}\,. \tag{2}$$

We take the Dirichlet trace of the representation formula to obtain the first boundary integral equation

$$\mathcal{V} q(\mathbf{x},\tau) - \left(\tfrac{I}{2} + \mathcal{K}\right) u(\mathbf{x},t) = 0\,, \qquad (\mathbf{x},t) \in \Gamma \times \Upsilon \tag{3}$$

with the thermal single- and double layer operator

$$\mathcal{V} q(\mathbf{x},t) := \int_0^t \int_\Gamma G(\mathbf{x} - \mathbf{y}, t - \tau) q(\mathbf{y},\tau) \mathrm{d}s_\mathbf{y} \mathrm{d}\tau\,, \tag{4}$$

$$\mathcal{K} u(\mathbf{x},t) := \int_0^t \int_\Gamma \partial_{n_\mathbf{y}} G(\mathbf{x} - \mathbf{y}, t - \tau) u(\mathbf{y},\tau) \mathrm{d}s_\mathbf{y} \mathrm{d}\tau\,. \tag{5}$$

Taking the Neumann trace of the representation formula yields the second boundary integral equation

$$\left(-\tfrac{I}{2}+\mathcal{K}'\right)q(\mathbf{x},t)+\mathcal{D}u(\mathbf{x},t)=0\,,\qquad(\mathbf{x},t)\in\Gamma\times\Upsilon \tag{6}$$

with the adjoint double layer- and the hypersingular operator

$$\mathcal{K}'q(\mathbf{x},t):=\int_0^t\int_\Gamma \partial_{n_\mathbf{x}}G(\mathbf{x}-\mathbf{y},t-\tau)q(\mathbf{y},\tau)\mathrm{d}s_\mathbf{y}\mathrm{d}\tau\,, \tag{7}$$

$$\mathcal{D}u(\mathbf{x},t):=-\partial_{n_\mathbf{x}}\int_0^t\int_\Gamma \partial_{n_\mathbf{y}}G(\mathbf{x}-\mathbf{y},t-\tau)u(\mathbf{y},\tau)\mathrm{d}s_\mathbf{y}\mathrm{d}\tau\,. \tag{8}$$

Similar to the case of elliptic equations, the bilinear form of the thermal hypersingular operator has a representation in terms of a weakly singular operator.

Theorem 2.1. *The bilinear form of the hypersingular operator can be represented by*

$$\begin{aligned}\langle\mathcal{D}u,v\rangle_{\Gamma\times\Upsilon}=&\int_0^T\int_\Gamma \mathbf{curl}_\mathbf{x}^\top v(\mathbf{x},t)\int_0^t\int_\Gamma G(\mathbf{x}-\mathbf{y},t-\tau)\mathbf{curl}_\mathbf{y}u(\mathbf{y},\tau)\,ds_\mathbf{y}d\tau\,ds_\mathbf{x}dt\\&-\lim_{\varepsilon\to0}\int_0^T\int_\Gamma \mathbf{n}_\mathbf{x}{}^\top v(\mathbf{x},t)\int_0^t\int_{\Gamma\setminus B_\varepsilon(\mathbf{x})}\partial_\tau G(\mathbf{x}-\mathbf{y},t-\tau)\mathbf{n}_\mathbf{y}u(\mathbf{y},\tau)\,ds_\mathbf{y}d\tau\,ds_\mathbf{x}dt\,,\end{aligned}$$

where $\mathbf{curl}_\mathbf{x}:=\mathbf{n}_\mathbf{x}\times\nabla_\Gamma$ *is the surface curl and* ∇_Γ *the surface gradient. Further,* $B_\varepsilon(\mathbf{x})$ *is a ball of radius* ε *centered in* $\mathbf{x}$.

The two dimensional version of this result is given in [4, Theorem 6.1]. In three dimensions the result can be shown with similar techniques as for the hypersingular operator of the Laplace equation, see, e.g., [12, proof of Theorem 6.17]. We omit the details.

2.2 Properties of Boundary Integral Operators

Recall that for positive r,s the $H^{r,s}(\Gamma\times\mathbb{R})$ norm is defined by

$$\|u\|^2_{H^{r,s}(\Gamma\times\mathbb{R})}=\int_\mathbb{R}\|\hat{u}(\cdot,\tau)\|^2_{H^r(\Gamma)}+\left(1+\tau^2\right)^s\|\hat{u}(\cdot,\tau)\|^2_{L_2(\Gamma)}\,\mathrm{d}\tau\,, \tag{9}$$

where $\hat{u}(\mathbf{x},\tau)$ is the Fourier transform of $u(\mathbf{x},t)$ in time, i.e.,

$$\hat{u}(\mathbf{x},\tau)=\frac{1}{\sqrt{2\pi}}\int_\mathbb{R}e^{-i\tau t}u(\mathbf{x},t)\mathrm{d}t\,.$$

The space $H^{r,s}(\Gamma\times\Upsilon)$ consists of functions in $H^{r,s}(\Gamma\times\mathbb{R})$ restricted to the interval Υ and is equipped with the quotient norm

$$\|u\|_{H^{r,s}(\Gamma\times\Upsilon)}=\inf_{\substack{U\in H^{r,s}(\Gamma\times\mathbb{R})\\U|_{\Gamma\times\Upsilon}=u}}\|U\|_{H^{r,s}(\Gamma\times\mathbb{R})}\,,$$

while the spaces of negative order are defined by duality, i.e., $H^{-r,-s}(\Gamma\times\Upsilon)=\left[H^{r,s}(\Gamma\times\Upsilon)\right]'$.

For an open part of the boundary surface $\Gamma_0\subset\Gamma$ the space $\widetilde{H}^{r,s}(\Gamma_0\times\Upsilon)$ is the closed subspace

$$\widetilde{H}^{r,s}(\Gamma_0\times\Upsilon):=\{u\in H^{r,s}(\Gamma\times\Upsilon)\,:\,\mathrm{supp}\,u\subset\Gamma_0\}$$

of $H^{r,s}(\Gamma\times\Upsilon)$.

Theorem 2.2. *[4, Theorems 3.10 and 3.11] The operator*

$$\mathcal{A}:=\begin{bmatrix}\mathcal{V} & -\mathcal{K}\\ \mathcal{K}' & \mathcal{D}\end{bmatrix}$$

is an isomorphism of the space $H^{-\frac12,-\frac14}(\Gamma\times\Upsilon)\times H^{\frac12,\frac14}(\Gamma\times\Upsilon)$ onto its dual space. Further, $\mathcal{A}$ is elliptic, i.e.,

$$\left\langle\mathcal{A}\begin{bmatrix}p\\ v\end{bmatrix},\begin{bmatrix}p\\ v\end{bmatrix}\right\rangle_{\Gamma\times\Upsilon}\gtrsim\|p\|^2_{H^{-\frac12,-\frac14}(\Gamma\times\Upsilon)}+\|v\|^2_{H^{\frac12,\frac14}(\Gamma\times\Upsilon)}\,.$$

Theorem 2.3. *[4, Theorem 4.8 and 4.16] On piecewise Lipschitz boundaries Γ the boundary integral operators*

$$\begin{aligned}\mathcal{V}&:H^{-\frac12+s,(-\frac12+s)/2}(\Gamma\times\Upsilon)\to H^{\frac12+s,(\frac12+s)/2}(\Gamma\times\Upsilon)\,,\\ \pm\tfrac{I}{2}+\mathcal{K}&:H^{\frac12+s,(\frac12+s)/2}(\Gamma\times\Upsilon)\to H^{\frac12+s,(\frac12+s)/2}(\Gamma\times\Upsilon)\,,\\ \pm\tfrac{I}{2}+\mathcal{K}'&:H^{-\frac12+s,(-\frac12+s)/2}(\Gamma\times\Upsilon)\to H^{-\frac12+s,(-\frac12+s)/2}(\Gamma\times\Upsilon)\,,\\ \mathcal{D}&:H^{\frac12+s,(\frac12+s)/2}(\Gamma\times\Upsilon)\to H^{-\frac12+s,(-\frac12+s)/2}(\Gamma\times\Upsilon)\end{aligned}$$

are isomorphisms for $s\in\left(-\frac12,\frac12\right)$.

We note that the single- and double layer operators are self-adjoint with respect to a time-twisted duality, i.e.,

$$\left\langle\mathcal{V}p,\mathcal{R}_Tq\right\rangle_{\Gamma\times\Upsilon}=\left\langle\mathcal{V}q,\mathcal{R}_Tp\right\rangle_{\Gamma\times\Upsilon}\quad\text{and}\quad\left\langle\mathcal{D}u,\mathcal{R}_Tv\right\rangle_{\Gamma\times\Upsilon}=\left\langle\mathcal{D}v,\mathcal{R}_Tu\right\rangle_{\Gamma\times\Upsilon}\,.$$

Likewise, the normal derivative of the single layer operator and the double layer operators satisfy

$$\left\langle\mathcal{K}v,\mathcal{R}_Tq\right\rangle_{\Gamma\times\Upsilon}=\left\langle\mathcal{K}'q,\mathcal{R}_Tv\right\rangle_{\Gamma\times\Upsilon}\,.$$

Here $\mathcal{R}_T$ is the time inversion operator $\mathcal{R}_Tv(\cdot,t)=v(\cdot,T-t)$, which is an isometry in $H^{r,s}(\Gamma\times\Upsilon)$.

The discussion below will depend on the mapping properties of the Dirichlet to Neumann map $\mathcal{S}$. We use the well known symmetric representation

$$\mathcal{S}u=\left[\mathcal{D}+\left(\tfrac12+\mathcal{K}'\right)\mathcal{V}^{-1}\left(\tfrac12+\mathcal{K}\right)\right]u\,. \tag{10}$$

Lemma 2.1. *The operator $\mathcal{S}$ is $H^{\frac12,\frac14}(\Gamma\times\Upsilon)$-elliptic and*

$$\mathcal{S}\,:\,H^{\frac12+s,(\frac12+s)/2}(\Gamma\times\Upsilon)\to H^{-\frac12+s,(-\frac12+s)/2}(\Gamma\times\Upsilon)$$

is an isomorphism for $s\in\left(-\frac12,\frac12\right)$.

Proof. For $u \in H^{\frac{1}{2},\frac{1}{4}}(\Gamma\times\Upsilon)$ write

$$\mathcal{S}u = \left(\tfrac{I}{2} + \mathcal{K}'\right) q + \mathcal{D}u\,,$$

where

$$\mathcal{V}q - \left(\tfrac{I}{2} + \mathcal{K}\right) u = 0$$

is in $H^{-\frac{1}{2},-\frac{1}{4}}(\Gamma\times\Upsilon)$. Multiplying the above equations by u and q gives

$$\langle \mathcal{S}u, u\rangle_{\Gamma\times\Upsilon} = \left\langle \begin{bmatrix} 0 \\ \mathcal{S}u \end{bmatrix}, \begin{bmatrix} q \\ u \end{bmatrix} \right\rangle_{\Gamma\times\Upsilon} = \left\langle \mathcal{A}\begin{bmatrix} q \\ u \end{bmatrix}, \begin{bmatrix} q \\ u \end{bmatrix} \right\rangle_{\Gamma\times\Upsilon}$$

where the $1/2$-terms have canceled. Because of the ellipticity of $\mathcal{A}$ it follows that

$$\langle \mathcal{S}u, u\rangle_{\Gamma\times\Upsilon} \gtrsim \|q\|^2_{H^{-\frac{1}{2},-\frac{1}{4}}(\Gamma\times\Upsilon)} + \|u\|^2_{H^{\frac{1}{2},\frac{1}{4}}(\Gamma\times\Upsilon)} \gtrsim \|u\|^2_{H^{\frac{1}{2},\frac{1}{4}}(\Gamma\times\Upsilon)}\,,$$

which implies the first assertion. The mapping properties of $\mathcal{S}$ follow directly from (10) and Theorem 2.3. A symmetric representation of the inverse can be derived by adding u to both sides of (3) and setting $u = \mathcal{S}^{-1}q$, where q is the Neumann data. Then

$$\mathcal{S}^{-1}q = \left[\mathcal{V} + \left(-\tfrac{I}{2} + \mathcal{K}\right)\mathcal{D}^{-1}\left(-\tfrac{I}{2} + \mathcal{K}'\right)\right] q\,. \tag{11}$$

Thus the mapping properties of $\mathcal{S}^{-1}$ follow again from Theorem 2.3. □

We will also need the mapping properties of the Dirichlet to Robin map, which can be expressed as $g_R = (\mathcal{S} + \kappa I)\, u$, where u is the Dirichlet data, g_R the Robin data, and $0 \le \kappa \in L_\infty(\Gamma\times\Upsilon)$.

Lemma 2.2. *The operator $(\mathcal{S} + \kappa I)$ is $H^{\frac{1}{2},\frac{1}{4}}(\Gamma\times\Upsilon)$-elliptic and*

$$\mathcal{S} + \kappa I : H^{\frac{1}{2}+s,(\frac{1}{2}+s)/2}(\Gamma\times\Upsilon) \to H^{-\frac{1}{2}+s,(-\frac{1}{2}+s)/2}(\Gamma\times\Upsilon)$$

is an isomorphism for $s \in \left(-\frac{1}{2}, \frac{1}{2}\right)$.

Proof. Since the pointwise multiplication $\kappa I : H^{\frac{1}{2},\frac{1}{4}}(\Gamma\times\Upsilon) \to L_2(\Gamma\times\Upsilon)$ is continuous and since $L_2(\Gamma\times\Upsilon)$ is a subspace of $H^{-\frac{1}{2},-\frac{1}{4}}(\Gamma\times\Upsilon)$, the ellipticity and mapping properties of $(\mathcal{S} + \kappa I)$ follow directly from those of $\mathcal{S}$ in Lemma 2.1. It remains to establish the continuity of the inverse. To that end, consider the operator equation $(\mathcal{S} + \kappa I)\, u = g_R$. Setting $q = \mathcal{S}u$, the equation turns into $\left(I + \kappa\mathcal{S}^{-1}\right) q = g_R$.

Note that $\kappa\mathcal{S}^{-1} : H^{-\frac{1}{2}+s,-\frac{1}{4}+\frac{s}{2}}(\Gamma\times\Upsilon) \to L_2(\Gamma\times\Upsilon)$ is continuous and therefore a compact operator in $H^{-\frac{1}{2}+s,-\frac{1}{4}+\frac{s}{2}}(\Gamma\times\Upsilon)$. Further, it follows from the ellipticity that the only solution to the homogeneous equation is $q = 0$. By the Fredholm alternative $q \in H^{-\frac{1}{2}+s,-\frac{1}{4}+\frac{s}{2}}(\Gamma\times\Upsilon)$ and by Lemma 2.1 $u \in H^{\frac{1}{2}+s,\frac{1}{4}+\frac{s}{2}}(\Gamma\times\Upsilon)$. Moreover,

$$\|u\|_{H^{\frac{1}{2}+s,\frac{1}{4}+\frac{s}{2}}(\Gamma\times\Upsilon)} \sim \|q\|_{H^{-\frac{1}{2}+s,-\frac{1}{4}+\frac{s}{2}}(\Gamma\times\Upsilon)} \sim \|g_R\|_{H^{-\frac{1}{2}+s,-\frac{1}{4}+\frac{s}{2}}(\Gamma\times\Upsilon)}\,.$$

□

For the following discussion it will be convenient to introduce the spaces

$$H^s := H^{-\frac{1}{2}+s,-\frac{1}{4}+\frac{s}{2}}(\Gamma\times\Upsilon)\times H^{\frac{1}{2}+s,\frac{1}{4}+\frac{s}{2}}(\Gamma\times\Upsilon) \tag{12}$$

for $s\in\left(-\frac{1}{2},\frac{1}{2}\right)$ which have norms

$$\|\phi\|_{H^s}^2 := \|q\|^2_{H^{-\frac{1}{2}+s,-\frac{1}{4}+\frac{s}{2}}(\Gamma\times\Upsilon)} + \|u\|^2_{H^{\frac{1}{2}+s,\frac{1}{4}+\frac{s}{2}}(\Gamma\times\Upsilon)}$$

where $\phi=[q,u]\in H^s$. The dual space is given by

$$(H^s)' := H^{\frac{1}{2}-s,\frac{1}{4}-\frac{s}{2}}(\Gamma\times\Upsilon)\times H^{-\frac{1}{2}-s,-\frac{1}{4}-\frac{s}{2}}(\Gamma\times\Upsilon).$$

Errors introduced by the fast evaluation of layer potentials will be estimated in the space $\check{H}$, defined by

$$\check{H} := L_2(\Gamma\times\Upsilon)\times H^{1,0}(\Gamma\times\Upsilon). \tag{13}$$

For a duality argument later on we will need the following result.

Lemma 2.3. *For $f=[f_D,f_R]\in(H^{-s})'$, $s\in\left(-\frac{1}{2},\frac{1}{2}\right)$ the system*

$$\begin{aligned}\mathcal{V}q-\left(\tfrac{I}{2}+\mathcal{K}\right)u &= f_D\\ \left(\tfrac{I}{2}+\mathcal{K}'\right)q+(\mathcal{D}+\kappa I)u &= f_R\end{aligned}$$

has a solution $\phi=[q,u]\in H^s$ and the norm equivalence $\|\phi\|_{H^s}\sim\|f\|_{(H^{-s})'}$ holds.

Proof. Simple elimination shows that

$$\begin{aligned}u &= (\mathcal{S}+\kappa I)^{-1}\left(f_R-\left(\tfrac{I}{2}+\mathcal{K}'\right)\mathcal{V}^{-1}f_D\right)\\ q &= \mathcal{V}^{-1}\left(\left(\tfrac{I}{2}+\mathcal{K}\right)u+f_D\right)\end{aligned}$$

The assertion follows directly from the mapping properties of the boundary integral operators in Theorem 2.3 and the Dirichlet to Robin map in Lemma 2.2. □

2.3 Boundary Integral Formulations

We now derive the boundary integral formulation of the mixed initial boundary value problem (1). For this purpose, we define the surfaces Γ_{DR} and Γ_{NR}, which are the interiors of $\overline{\Gamma}_D\cup\overline{\Gamma}_R$ and $\overline{\Gamma}_N\cup\overline{\Gamma}_R$, respectively. Further, we assume that the Dirichlet- and Neumann data have extensions $\tilde{g}_D\in H^{\frac{1}{2},\frac{1}{4}}(\Gamma\times\Upsilon)$ and $\tilde{g}_N\in H^{-\frac{1}{2},-\frac{1}{4}}(\Gamma\times\Upsilon)$ to all of $\Gamma\times\Upsilon$. Thus the Dirichlet- and Neumann data can be written as $u=\tilde{u}+\tilde{g}_D$ and $q=\tilde{q}+\tilde{q}_N$ with unknown $\tilde{u}\in\widetilde{H}^{\frac{1}{2},\frac{1}{4}}(\Gamma_{NR}\times\Upsilon)$ and $\tilde{q}\in\widetilde{H}^{-\frac{1}{2},-\frac{1}{4}}(\Gamma_{DR}\times\Upsilon)$. Moreover, define

$$\kappa_R(\mathbf{x},t) := \begin{cases}\kappa(\mathbf{x},t), & (\mathbf{x},t)\in\Gamma_R\times\Upsilon,\\ 0, & (\mathbf{x},t)\in\Gamma_N\times\Upsilon,\end{cases} \text{ and } f_R(\mathbf{x},t) := \begin{cases}g_R(\mathbf{x},t), & (\mathbf{x},t)\in\Gamma_R\times\Upsilon,\\ 0, & (\mathbf{x},t)\in\Gamma_N\times\Upsilon.\end{cases}$$

To determine $\tilde{u}, \tilde{q}$ we choose the following system of boundary integral equations based upon the first and second Green's formula (3) and (6)

$$\begin{aligned} \mathcal{V}(\tilde{q}+\tilde{g}_N)(\mathbf{x},t) - \left(\tfrac{I}{2}+\mathcal{K}\right)(\tilde{u}+\tilde{g}_D)(\mathbf{x},t) = 0\,, &\qquad (\mathbf{x},t)\in\Gamma_{DR}\times\Upsilon,\\ \left(\tfrac{I}{2}+\mathcal{K}'\right)(\tilde{q}+\tilde{g}_N)(\mathbf{x},t) + (\mathcal{D}+\kappa_R I)(\tilde{u}+\tilde{g}_D)(\mathbf{x},t) = f_R(\mathbf{x},t)\,, &\quad (\mathbf{x},t)\in\Gamma_{NR}\times\Upsilon. \end{aligned}$$

If $\Gamma_R = \emptyset$ then this formulation reduces to the well known symmetric formulation of the mixed Dirichlet-Neumann problem.

We state the variational form of this problem in a slightly more general setting. To that end, let $f \in \left(H^0\right)'$ and $g \in H^0$ be given, further, let V be a closed subspace of H^0. Consider the variational problem: Find $\phi \in V$ such that for all $\chi \in V$

$$a(\phi+g,\chi) = \langle f,\chi\rangle\,. \tag{14}$$

Here, $\langle\cdot,\cdot\rangle$ denotes the $L_2(\Gamma\times\Upsilon)$-duality pairing and the bilinear form is

$$a(\psi,\chi) = \left\langle \mathcal{V}q,p\right\rangle - \left\langle \left(\tfrac{I}{2}+\mathcal{K}\right)u,p\right\rangle + \left\langle \left(\tfrac{I}{2}+\mathcal{K}'\right)q,v\right\rangle + \left\langle (\mathcal{D}+\kappa_R I)\,u,v\right\rangle, \tag{15}$$

where $\psi = \phi + g = [q,u] \in H^0$ and $\chi = [p,v] \in H^0$. Since the $1/2$-terms cancel, it follows from Theorem 2.2 that $a(\cdot,\cdot)$ is coercive and bounded in H^0 and therefore coercive and bounded in the subspace V. Thus (14) is well-posed.

For the mixed problem we have $V = \widetilde{H}^{-\frac{1}{2},-\frac{1}{4}}(\Gamma_{DR}\times\Upsilon)\times\widetilde{H}^{\frac{1}{2},\frac{1}{4}}(\Gamma_{NR}\times\Upsilon)$, $\phi = [\tilde{q},\tilde{u}]$ $g = [\tilde{g}_N,\tilde{g}_D]$ and $f = [0,f_R]$. We note, however, that (14) also includes the pure Dirichlet, Neumann, and Robin initial boundary value problems as special cases, thus the ensuing error analysis also applies to these problems as well. Since their numerical formulations can be significantly simpler, we list them below.

2.3.1 Initial Dirichlet Boundary Value Problem

For the pure Dirichlet problem of the heat equation (1) we have $\Gamma_D = \Gamma$, $\Gamma_N = \Gamma_R = \emptyset$. In this case the first boundary integral equation (3) can be used as a boundary integral formulation

$$\mathcal{V}q(\mathbf{x},t) = \left(\tfrac{I}{2}+\mathcal{K}\right)g_D(\mathbf{x},t)\,, \qquad (\mathbf{x},t)\in\Gamma\times\Upsilon. \tag{16}$$

The variational formulation of this problem is given by (14) with $V = H^{-\frac{1}{2},-\frac{1}{4}}(\Gamma\times\Upsilon)\times\{0\}$, $\phi = [q,0]$, $g = [0,g_D]$, and $f = 0$.

2.3.2 Initial Neumann Boundary Value Problem

When $\Gamma_N = \Gamma$, $\Gamma_D = \Gamma_R = \emptyset$, then the second boundary integral equation (6) can be used to obtain a boundary integral formulation

$$\mathcal{D}u(\mathbf{x},t) = \left(\tfrac{I}{2}-\mathcal{K}'\right)g_N(\mathbf{x},t)\,, \qquad (\mathbf{x},t)\in\Gamma\times\Upsilon\,. \tag{17}$$

The variational form can be obtained by setting $V = \{0\}\times H^{-\frac{1}{2},-\frac{1}{4}}(\Gamma\times\Upsilon)$, $\phi = [0,u]$, $g = [0,g_N]$, $\kappa = 0$ and $f = [0,g_R]$.

2.3.3 Initial Robin Boundary Value Problem

The pure Robin problem is characterized by $\Gamma_R = \Gamma$, $\Gamma_D = \Gamma_R = \emptyset$. Similar to [12, page 181] we use the symmetric representation of Dirichlet to Robin map given in Lemma 2.2

$$(\mathcal{S} + \kappa_R I)\, u(\mathbf{x},t) = g_R(\mathbf{x},t)\,, \qquad (\mathbf{x},t) \in \Gamma \times \Upsilon\,.$$

Because of the inverse single layer operator in the definition of $\mathcal{S}$ it is difficult to realize this equation numerically. Therefore, we introduce the Neumann data $q = \mathcal{V}^{-1}\left(\frac{I}{2} + \mathcal{K}\right) u$ as an additional unknown and solve the equivalent system

$$\begin{aligned} \mathcal{V} q(\mathbf{x},t) - \left(\tfrac{I}{2} + \mathcal{K}\right) u(\mathbf{x},t) &= 0\,, && (\mathbf{x},t) \in \Gamma \times \Upsilon\,, \\ \left(\tfrac{I}{2} + \mathcal{K}'\right) q(\mathbf{x},t) + (\mathcal{D} + \kappa_R I)\, u(\mathbf{x},t) &= g_R(\mathbf{x},t)\,, && (\mathbf{x},t) \in \Gamma \times \Upsilon\,. \end{aligned} \tag{18}$$

The variational form of this problem is again (14) where $V = H^0$, $g = 0$, and $f = [0, g_R]$.

3 Galerkin Boundary Element Method

3.1 Properties of the Space-Time Tensor-Product Spaces

Throughout this work we assume a quasi-uniform, conforming triangulation of the boundary Γ and an equidistant partition of the time interval Υ. Further, we assume the interior of every triangle is entirely contained in either Γ_D, Γ_N or Γ_R. Upon this triangulation we define piecewise polynomial ansatz spaces of degree d_x in space (either piecewise constant $d_x = d_0$ or piecewise linear and continuous $d_x = c_1$)

$$X_{h_x}^{d_x}(\Gamma) := \operatorname{span}\{\varphi_{h_x,\ell}^{d_x}(\mathbf{x})\}_{\ell=0}^{N_x-1}\,.$$

Here, $\varphi_{h_x,\ell}^{d_0}$ is the characteristic function of the ℓ-th triangle and $\varphi_{h_x,\ell}^{c_1}$ a hat-function corresponding to the ℓ-th vertex. Further, N_x is the number of triangles when $d_x = d_0$ or the number of vertices when $d_x = c_1$. For the time variable we consider a piecewise constant ansatz space

$$T_{h_t}^{d_t}(\Upsilon) := \operatorname{span}\{\phi_{h_t,j}^{d_0}(t)\}_{j=0}^{N_t-1}\,,$$

where $\phi_{h_t,j}^{d_0}$ is the characteristic function of the j-th time interval and N_t the number of time steps. Note that $\phi_{h_t,j}^{d_0}(t) = \phi_{\mathrm{loc}}(t/h - j)$, where ϕ_{loc} is the characteristic function of the interval $[0,1]$. To discretize functions in space and time we construct the tensor-product spaces

$$V_{h_x,h_t}^{d_x,d_t}(\Gamma \times \Upsilon) := X_{h_x}^{d_x}(\Gamma) \otimes T_{h_t}^{d_t}(\Upsilon)\,,$$

thus the lowest order H^0-conforming ansatz space is

$$V_h(\Gamma \times \Upsilon) := V_{h_x,h_t}^{d_0,d_0}(\Gamma \times \Upsilon) \times V_{h_x,h_t}^{c_1,d_0}(\Gamma \times \Upsilon)\,.$$

Theorem 3.1. *[4, Proposition 5.3] Let $d_x = d_0$ or $d_x = c_1$ and $d_t = d_0$. Then the $L_2(\Gamma\times\Upsilon)$ projection, defined by*

$$\langle w - \mathcal{P}_{h_x}^{d_x}\mathcal{P}_{h_t}^{d_t} w, w_h\rangle_{L_2(\Gamma\times\Upsilon)} = 0 \qquad \forall w_h \in V_{h_x,h_t}^{d_x,d_t}(\Gamma\times\Upsilon)\,,$$

satisfies

$$\left\| w - \mathcal{P}_{h_x}^{d_x}\mathcal{P}_{h_t}^{d_t} w \right\|_{H^{s_x,s_t}(\Gamma\times\Upsilon)} \lesssim \left(h_x^{\alpha} + h_t^{\beta}\right) \|w\|_{H^{r_x,r_t}(\Gamma\times\Upsilon)}$$

for $w \in H^{r_x,r_t}(\Gamma\times\Upsilon)$, where $s_x s_t \geq 0$, $s_x \leq r_x$, $s_t \leq r_t$, $r_t \leq 1$, $s_t < \frac{1}{2}$,

$$r_x \leq \begin{cases} 1, & d_x = d_0, \\ 2, & d_x = c_1, \end{cases} \qquad s_x < \begin{cases} \frac{1}{2}, & d_x = d_0, \\ \frac{3}{2}, & d_x = c_1, \end{cases}$$

and

$$\alpha = \min\left\{ r_x - s_x, r_x - \frac{r_x}{r_t} s_t \right\}, \qquad \beta = \min\left\{ r_t - s_t, r_t - \frac{r_t}{r_x} s_x \right\}.$$

A simple consequence of this result is

Corollary 3.1. *The $L_2(\Gamma\times\Upsilon)$ projection $\mathcal{P}_h : [q,u] \to [\mathcal{P}_{h_x}^{d_0}\mathcal{P}_{h_t}^{d_0} q, \mathcal{P}_{h_x}^{c_1}\mathcal{P}_{h_t}^{d_0} u]$ satisfies*

$$\|\chi - \mathcal{P}_h\chi\|_{H^s} \lesssim \left(h_x^{r-s} + h_t^{\frac{r-s}{2}}\right) \|\chi\|_{H^r}\,,$$
$$\|\chi - \mathcal{P}_h\chi\|_{\check{H}} \lesssim \left(h_x^{r-\frac{1}{2}} + h_t^{\frac{r}{2}-\frac{1}{4}}\right) \|\chi\|_{H^r}$$

for $\chi \in H^r$, $0 \leq r \leq \frac{3}{2}$, $s \leq r$ and $0 \leq s < \frac{1}{2}$.

Corollary 3.2. *The L_2 projection satisfies the stability conditions*

$$\|\mathcal{P}_h\chi\|_{H^s} \lesssim \|\chi\|_{H^s}\,, \quad 0 \leq s < \frac{1}{2}\,,$$
$$\|\mathcal{P}_h\chi\|_{\check{H}} \lesssim \|\chi\|_{H^{\frac{1}{2}}}\,.$$

Proof. The triangle inequality and Corollary 3.1 for $r = s$ lead to

$$\|\mathcal{P}_h\chi\|_{H^s} \leq \|\chi - \mathcal{P}_h\chi\|_{H^s} + \|\chi\|_{H^s} \lesssim \|\chi\|_{H^s}\,.$$

For the second assertion replace H^s by $\check{H}$ and use $\|\chi\|_{\check{H}} \leq \|\chi\|_{H^{\frac{1}{2}}}$. □

Theorem 3.2. *The following inverse inequalities*

$$\|p_h\|_{H^{-s_x,-s_t}(\Gamma\times\Upsilon)} \lesssim \left(h_x^{-(r_x-s_x)} + h_t^{-(r_t-s_t)}\right) \|p_h\|_{H^{-r_x,-r_t}(\Gamma\times\Upsilon)}\,, \qquad 0 \leq s_x \leq r_x \leq \frac{1}{2},\ 0 \leq s_t \leq r_t \leq \frac{1}{2},$$

$$\|v_h\|_{H^{r_x,r_t}(\Gamma\times\Upsilon)} \lesssim \left(h_x^{-(r_x-s_x)} + h_t^{-(r_t-s_t)}\right) \|v_h\|_{H^{s_x,s_t}(\Gamma\times\Upsilon)}\,, \qquad 0 \leq s_x \leq r_x < \frac{3}{2},\ 0 \leq s_t \leq r_t < \frac{1}{2},$$

hold for all $p_h \in V_{h_x,h_t}^{d_0,d_0}(\Gamma\times\Upsilon)$ and $v_h \in V_{h_x,h_t}^{c_1,d_0}(\Gamma\times\Upsilon)$.

For positive order, these inverse estimates follow directly from the well-known inverse estimates in the spaces $X_{h_x}^{d_x}(\Gamma)$ and $T_{h_t}^{d_t}(\Upsilon)$, see [9, Lemma 7.4]. The estimates for negative order can be obtained with a duality argument, see, e.g.,[12, Lemma 10.10]. We omit details.

Corollary 3.3. *The following inverse inequalities*

$$\begin{aligned} \|\chi_h\|_{H^s} &\lesssim \left(h_x^{-s} + h_t^{-\frac{s}{2}}\right) \|\chi_h\|_{H^0}\,, && 0 \le s < \frac{1}{2}, \\ \|\chi_h\|_{\check{H}} &\lesssim \left(h_x^{-\frac{1}{2}+s} + h_t^{-\frac{1}{4}+\frac{s}{2}}\right) \|\chi_h\|_{H^s}\,, && 0 \le s < \frac{1}{2}, \end{aligned}$$

hold for all $\chi_h \in V_{h_x,h_t}^{d_0,d_0}(\Gamma\times\Upsilon) \times V_{h_x,h_t}^{c_1,d_0}(\Gamma\times\Upsilon)$.

3.2 Efficient Solution Procedure

To describe the Galerkin discretization of (14), we introduce the finite element space

$$V_h = V \cap \left(V_{h_x,h_t}^{d_0,d_0}(\Gamma\times\Upsilon) \times V_{h_x,h_t}^{c_1,d_0}(\Gamma\times\Upsilon)\right)$$

and the projection $g_h = [g_{N,h}, g_{D,h}]$ where $g_{N,h} = \mathcal{P}_{h_x}^{d_0}\mathcal{P}_{h_t}^{d_0} g_N$ and $g_{D,h} = \mathcal{P}_{h_x}^{c_1}\mathcal{P}_{h_t}^{d_0} g_D$. This approximation is necessary to avoid a separate quadrature to compute the application of boundary integral operators to the Dirichlet or Neumann data. Thus the discrete problem is: Find $\phi_h \in V_h$ such that for all $\chi_h \in V_h$

$$a(\phi_h + g_h, \chi_h) = \langle f, \chi_h\rangle\,. \tag{19}$$

The discrete problem appears in the form of a lower-triangular block-Töplitz system,

$$\sum_{j=0}^{i} \mathsf{A}_{i-j}\psi_j = \mathsf{f}_i\,, \qquad i = 0,\dots N_t - 1.$$

Here ψ_j and f_j are coefficient vectors of the solution and right hand side for time step j and

$$\mathsf{A}_i = \begin{bmatrix} \mathsf{V}_i & -\left(\frac{\delta_{0,i}}{2}\mathsf{M} + \mathsf{K}_i\right) \\ \left(\frac{\delta_{0,i}}{2}\mathsf{M}^\top + \mathsf{K}_i^\top\right) & \mathsf{D}_{\kappa,\mathsf{i}} \end{bmatrix},$$

where the blocks correspond to the different layer potentials

$$[\mathsf{V}_i]_{k,\ell} = \int_\Gamma \int_\Gamma V_{h_t,i}(\mathbf{x}-\mathbf{y})\varphi_{h_x,k}^{d_0}(\mathbf{x})\varphi_{h_x,\ell}^{d_0}(\mathbf{y})\mathrm{d}s_\mathbf{y}\mathrm{d}s_\mathbf{x}.$$

The time integrated kernel are given by

$$V_{h_t,i-j}(\mathbf{x}-\mathbf{y}) = \begin{cases} \int_{t=0}^{h_t}\int_{\tau=0}^{t} G(\mathbf{x}-\mathbf{y},t-\tau)\phi_{h_t,i}^{d_0}(t)\phi_{h_t,j}^{d_0}(\tau)\mathrm{d}\tau\mathrm{d}t\,, & i = j\,, \\ \int_{t=0}^{h_t}\int_{\tau=0}^{h_t} G(\mathbf{x}-\mathbf{y},t-\tau)\phi_{h_t,i}^{d_0}(t)\phi_{h_t,j}^{d_0}(\tau)\mathrm{d}\tau\mathrm{d}t\,, & i > j\,. \end{cases} \tag{20}$$

The matrices K_i and $\mathsf{D}_{\kappa,\mathsf{i}}$ are defined similarly for the double layer operator and the operator $\mathcal{D}+\kappa_R I$. Finally, $\delta_{i,j}$ is the Kronecker-delta and M is the mass matrix

$$\mathsf{M}_{k,\ell} = h_t \int_\Gamma \varphi^{d_0}_{h_x,k}(\mathbf{x})\varphi^{c_1}_{h_x,\ell}(\mathbf{x})\mathrm{d}s_{\mathbf{x}} \,.$$

The solution of the above system can be found by forward elimination, where every time step amounts to solving

$$\mathsf{A}_0\phi_i = \mathsf{b}_i \,, \quad i = 0,\ldots N_t - 1 \,, \tag{21}$$

where the right hand side involves the solution of the previous time steps

$$\mathsf{b}_i = \mathsf{f}_i - \sum_{j=0}^{i-1} \mathsf{A}_{i-j}\phi_j \,.$$

This linear system can be solved by elimination; writing $\mathsf{b}_i = [\mathsf{c},\mathsf{d}]$ and $\phi_i = [\mathsf{q},\mathsf{u}]$ we have

$$\mathsf{S}_0\,\mathsf{u} = \mathsf{d} - \left(\frac{1}{2}\mathsf{M}+\mathsf{K}_0\right)^\top \mathsf{V}_0^{-1}\mathsf{c} \,, \tag{22}$$

$$\mathsf{V}_0\,\mathsf{q} = \mathsf{c} + \left(\frac{1}{2}\mathsf{M}+\mathsf{K}_0\right)\mathsf{u} \,, \tag{23}$$

where S_0 is given by

$$\mathsf{S}_0 = \mathsf{D}_{\kappa,0} + \left(\frac{1}{2}\mathsf{M}+\mathsf{K}_0\right)^\top \mathsf{V}_0^{-1}\left(\frac{1}{2}\mathsf{M}+\mathsf{K}_0\right) \tag{24}$$

which can be viewed as a discrete Dirichlet to Robin operator. Thus every time step involves solving linear systems with V_0 and S_0.

Note that the matrices on the left and right hand side are dense and must be evaluated by a fast method to overcome a complexity estimate that grows quadratically with the number of unknowns. This is achieved by an adaption of the parabolic fast multipole algorithm (pFMM) [13], [14] to Galerkin discretized boundary integral operators of the heat equation as described in [7] and [6].

4 Error Estimates

Error estimates for the Galerkin discretization of boundary integral equations of parabolic integral equation were already derived in [4, 9]. However, the discussion there assumes that the boundary data and the bilinear form of the operators are represented exactly. To account for their approximations, a variation of the well known Strang lemma and the Aubin-Nitsche duality argument can be used. To make this work self contained we will give the argument in this section, while for a discussion along these lines in the case of elliptic BEM we refer to [10].

When multiplying powers of the temporal and spatial meshwidths we frequently use the following estimate which is a simple consequence of Young's inequality

$$\left(h_x^r + h_t^{\frac{r}{2}}\right)\left(h_x^s + h_t^{\frac{s}{2}}\right) \lesssim \left(h_x^{r+s} + h_t^{\frac{r+s}{2}}\right) \,, \quad rs \geq 0 \,.$$

If the exponents have opposite signs, then the product can be estimated by

$$\left(h_x^r + h_t^{\frac{r}{2}}\right)\left(h_x^{-s} + h_t^{-\frac{s}{2}}\right) \lesssim \mathcal{C}^s(h)\left(h_x^{r-s} + h_t^{\frac{r-s}{2}}\right), \quad r,s \geq 0\,,$$

where

$$\mathcal{C}(h) = \max\left\{\frac{h_x}{\sqrt{h_t}}, \frac{\sqrt{h_t}}{h_x}\right\}.$$

4.1 Bilinear Form

As mentioned in the introduction, we use the parabolic fast multipole method to evaluate layer potentials efficiently. This algorithm is based on a hierarchical subdivision of space-time into space-time clusters. To compute interactions of these clusters efficiently, the kernel (2) is approximated by an expression that separates the $(\mathbf{x},t)$ and $(\mathbf{y},\tau)$ variables, for instance, by a multivariate Chebyshev interpolation. This replaces the kernel by an approximation G_{ap} with error [14]

$$\left|G(\mathbf{x}-\mathbf{y},t-\tau) - G_{\text{ap}}(\mathbf{x}-\mathbf{y},t,\tau)\right| \lesssim h_t^{-\frac{3}{2}}\left(\rho_t^{p_t} + \rho_x^{p_x}\right) := \varepsilon_h\,, \tag{25}$$

where p_x and p_t are the expansion orders and $\rho_t < 1$ and $\rho_x < 1$ depend on the way the space-time clusters are separated with respect to their size. The point is that any desired accuracy ε_h can be achieved by increasing the expansion order, while the complexity of the fast algorithm is order $\left(p_t^2 + p_x^4\right)/(h_x^2 h_t)$, see [13, 7]. The subscript of ε_h indicates that the expansion orders are adjusted to the discretization mesh width, such that the approximation error of the kernel does not affect the asymptotic convergence of the discretization scheme.

For $\chi_h = [p_h, v_h]$ and $\phi_h = [q_h, u_h]$ in V_h the errors of the layer potentials when G is replaced by G_{ap} can be bounded as

$$\begin{aligned}
\left\langle (\mathcal{V} - \mathcal{V}_h)\, q_h, p_h\right\rangle_{\Gamma\times\Upsilon} &\lesssim \varepsilon_h \left\|q_h\right\|_{L_2(\Gamma\times\Upsilon)} \left\|p_h\right\|_{L_2(\Gamma\times\Upsilon)}\,,\\
\left\langle (\mathcal{K} - \mathcal{K}_h)\, u_h, p_h\right\rangle_{\Gamma\times\Upsilon} &\lesssim \varepsilon_h \left\|u_h\right\|_{H^{1,0}(\Gamma\times\Upsilon)} \left\|p_h\right\|_{L_2(\Gamma\times\Upsilon)}\,,\\
\left\langle \left(\mathcal{K}' - \mathcal{K}_h'\right) q_h, v_h\right\rangle_{\Gamma\times\Upsilon} &\lesssim \varepsilon_h \left\|q_h\right\|_{L_2(\Gamma\times\Upsilon)} \left\|v_h\right\|_{H^{1,0}(\Gamma\times\Upsilon)}\,,\\
\left\langle (\mathcal{D} - \mathcal{D}_h)\, u_h, v_h\right\rangle_{\Gamma\times\Upsilon} &\lesssim \varepsilon_h \left\|u_h\right\|_{H^{1,0}(\Gamma\times\Upsilon)} \left\|v_h\right\|_{H^{1,0}(\Gamma\times\Upsilon)}.
\end{aligned}$$

We will denote the resulting approximate bilinear form by $a_h(\cdot,\cdot)$. The variational problem we solve is: Find $\phi_h^* \in V_h$ such that for all $\chi_h \in V_h$

$$a_h(\phi_h^* + g_h, \chi_h) = \langle f, \chi_h\rangle\,. \tag{26}$$

In the remainder of this section we will derive error estimates for $\phi_h^* - \phi$. First note that the difference of the exact and approximate bilinear form satisfies the bound

$$|a(\phi_h,\chi_h) - a_h(\phi_h,\chi_h)| \lesssim \varepsilon_h \left\|\phi_h\right\|_{\check{H}} \left\|\chi_h\right\|_{\check{H}}\,, \tag{27}$$

where the space $\check{H}$ was introduced in (13). Using the inverse inequality (Corollary 3.3) and the ellipticity of $a(\cdot,\cdot)$ we can now estimate

$$\begin{aligned}
a_h(\chi_h,\chi_h) &= a(\chi_h,\chi_h) - \Big(a(\chi_h,\chi_h) - a_h(\chi_h,\chi_h)\Big)\\
&\gtrsim \left(1 - \varepsilon_h\left(h_x^{-1} + h_t^{-\frac{1}{2}}\right)\right)\left\|\chi_h\right\|_{H^0}^2
\end{aligned}$$

for all $\chi_h \in V_h$. Thus the approximate bilinear form $a_h(\cdot,\cdot)$ is coercive in V_h, independent of the mesh width, if ε_h goes to zero sufficiently fast, i.e.,

$$\varepsilon_h = o\left(\left(h_x^{-1} + h_t^{-\frac{1}{2}}\right)^{-1}\right).$$

To ensure that the fast method reproduces the full convergence behavior as the direct Galerkin discretization method the parameter ε_h must satisfy the stronger bound

$$\varepsilon_h \lesssim \mathcal{C}^{-\frac{1}{2}}(h)\left(h_x^2 + h_t^1\right), \tag{28}$$

which will become apparent in the following error estimates. Equation (25) implies that the expansion orders p_x and p_t depend logarithmically on the mesh width and hence, the complexity of the fast method is log-linear.

4.2 Estimates in the Energy Norm

The error in the H^0-norm can be estimated by the well known Strang Lemma (see, e.g., [2]).

Lemma 4.1. *If ε_h satisfies* (28) *and $\frac{1}{2} \le r \le \frac{3}{2}$ then the error of* (26) *can be estimated by*

$$\|\phi + g - \phi_h^* - g_h\|_{H^0} \lesssim \left(h_x^r + h_t^{\frac{r}{2}}\right)\|\phi + g\|_{H^r}.$$

Proof. For any $\chi_h \in V_h$ we set $\psi_h = \phi_h^* - \chi_h$ and estimate, using the ellipticity of $a_h(\cdot,\cdot)$

$$\begin{aligned}\|\phi_h^* - \chi_h\|_{H^0}^2 &\lesssim a_h(\phi_h^* - \chi_h, \phi_h^* - \chi_h)\\ &= a(\phi + g - \chi_h - g_h, \psi_h) + \left[a(\chi_h + g_h, \psi_h) - a_h(\chi_h + g_h, \psi_h)\right]\\ &\quad + \left[a_h(\phi_h^* + g_h, \psi_h) - a(\phi + g, \psi_h)\right].\end{aligned}$$

Because of (14) and (26) the last square bracket cancels and thus it follows from (27) and the boundedness of the bilinear form that

$$\|\phi_h^* - \chi_h\|_{H^0} \lesssim \|\phi + g - \chi_h - g_h\|_{H^0} + \varepsilon_h \|\chi_h + g_h\|_{\check{H}} \frac{\left\|\phi_h^* - \chi_h\right\|_{\check{H}}}{\left\|\phi_h^* - \chi_h\right\|_{H^0}}.$$

Setting $\chi_h = \mathcal{P}_h\phi$, and applying the inverse estimate gives

$$\|\phi_h^* - \mathcal{P}_h\phi\|_{H^0} \lesssim \|\phi + g - \mathcal{P}_h(\phi - g)\|_{H^0} + \varepsilon_h\left(h_x^{-\frac{1}{2}} + h_t^{-\frac{1}{4}}\right)\|\mathcal{P}_h(\phi + g)\|_{\check{H}}.$$

Combining this with the triangle inequality

$$\begin{aligned}\|\phi + g - \phi_h^* - g_h\|_{H^0} &\le \|\phi + g - \mathcal{P}_h(\phi + g)\|_{H^0} + \|\phi_h^* - \mathcal{P}_h\phi\|_{H^0}\\ &\lesssim \left(h_x^r + h_t^{\frac{r}{2}}\right)\|\phi + g\|_{H^r} + \varepsilon_h\left(h_x^{-\frac{1}{2}} + h_t^{-\frac{1}{4}}\right)\|\phi + g\|_{H^{\frac{1}{2}}},\end{aligned}$$

where we have used the approximation and stability properties of $\mathcal{P}_h$. The assertion follows from (28). □

4.3 Estimates in Stronger Norms

Error estimates in H^s-norms, $s > 0$, can be derived with the help of the inverse estimate.

Lemma 4.2. *If ε_h satisfies* (28)*, $s \in \left(0, \frac{1}{2}\right)$, and $r \in \left[\frac{1}{2}, \frac{3}{2}\right]$, then the error of* (26) *can be estimated by*

$$\|\phi + g - \phi_h^* - g_h\|_{H^s} \lesssim C^s(h) \left(h_x^{r-s} + h_t^{\frac{r-s}{2}}\right) \|\phi + g\|_{H^r} .$$

Moreover, the solution is stable in the sense that

$$\|\phi_h^* + g_h\|_{\breve{H}} \lesssim C^{\frac{1}{2}}(h) \|\phi + g\|_{H^{\frac{1}{2}}} .$$

Proof. From the triangle inequality, the approximation properties of $\mathcal{P}_h$ (Theorem 3.1), and the inverse estimate (Corollary 3.3) we get

$$\begin{aligned}\|\phi + g - \phi_h^* - g_h\|_{H^s} &\leq \|\phi + g - \mathcal{P}_h\phi - g_h\|_{H^s} + \|\mathcal{P}_h\phi - \phi_h^*\|_{H^s} \\ &\lesssim \left(h_x^{r-s} + h_t^{\frac{r-s}{2}}\right) \|\phi + g\|_{H^r} + \left(h_x^{-s} + h_t^{-\frac{s}{2}}\right) \|\mathcal{P}_h(\phi + g - \phi_h^* - g_h)\|_{H^0} ,\end{aligned}$$

where the last step is justified because $\mathcal{P}_h(g - g_h) = 0$. The stability of $\mathcal{P}_h$ (Corollary 3.2) and Lemma 4.1 then imply that

$$\|\phi + g - \phi_h^* - g_h\|_{H^s} \lesssim \left[\left(h_x^{r-s} + h_t^{\frac{r-s}{2}}\right) + \left(h_x^r + h_t^{\frac{r}{2}}\right)\left(h_x^{-s} + h_t^{-\frac{s}{2}}\right)\right] \|\phi + g\|_{H^r}$$

which gives the first assertion. To show the second statement, repeat the same arguments from before with H^s replaced by $\breve{H}$. This implies that

$$\|\phi + g - \phi_h^* - g_h\|_{\breve{H}} \leq C^{\frac{1}{2}}(h) \left(h_x^{r-\frac{1}{2}} + h_t^{\frac{r}{2}-\frac{1}{4}}\right) \|\phi + g\|_{H^{\frac{1}{2}}} .$$

Combining this result for $r = \frac{1}{2}$ with the triangle inequality leads to

$$\|\phi_h^* + g_h\|_{\breve{H}} \leq \|\phi + g - \phi_h^* - g_h\|_{\breve{H}} + \|\phi + g\|_{\breve{H}} \lesssim C^{\frac{1}{2}}(h) \|\phi + g\|_{H^{\frac{1}{2}}} ,$$

which is the second assertion. □

4.4 Estimates in Weaker Norms

The error in the H^{-s}-norm can be estimated with a variation of the Aubin-Nitsche duality argument.

Lemma 4.3. *If ε_h satisfies* (28)*, $\frac{1}{2} \leq r \leq \frac{3}{2}$ and $0 < s < \frac{1}{2}$ then the error of* (26) *can be estimated by*

$$\|\phi + g - \phi_h^* - g_h\|_{H^{-s}} \lesssim \left(h_x^{r+s} + h_t^{\frac{r+s}{2}}\right) \|\phi + g\|_{H^r} .$$

Proof. For $b \in (H^{-s})'$ let $\psi^b \in H^s$ be the solution of the adjoint problem

$$a(\chi, \psi^b) = \langle \chi, b \rangle , \quad \forall \chi \in H^0 . \tag{29}$$

Set $\chi = \phi + g - \phi_h^* - g_h$ in (29) and add and subtract $\mathcal{P}_h \psi^b \in V_h$. Then

$$\begin{aligned} \langle \phi + g - \phi_h^* - g_h, b \rangle &= a(\phi + g - \phi_h^* - g_h, \psi^b) \\ &= a(\phi + g - \phi_h^* - g_h, \psi^b - \mathcal{P}_h \psi^b) \\ &\quad + \left[a_h(\phi_h^* + g_h, \mathcal{P}_h \psi^b) - a(\phi_h^* + g_h, \mathcal{P}_h \psi^b) \right] \\ &\quad + \left[a(\phi + g, \mathcal{P}_h \psi^b) - a_h(\phi_h^* + g_h, \mathcal{P}_h \psi^b) \right] \end{aligned}$$

Since ϕ and ϕ_h^* solve (14) and (26) the second square bracket cancels, and thus

$$\begin{aligned} \|\phi + g - \phi_h^* - g_h\|_{H^{-s}} &= \sup_{b \in (H^{-s})'} \frac{\left\langle \phi + g - \phi_h^* - g_h, b \right\rangle}{\|b\|_{(H^{-s})'}} \\ &\lesssim \sup_{b \in (H^{-s})'} \left[\frac{a(\phi + g - \phi_h^* - g_h, \psi^b - \mathcal{P}_h \psi^b)}{\|b\|_{(H^{-s})'}} \right. \\ &\qquad \left. + \frac{a_h(\phi_h^* + g_h, \mathcal{P}_h \psi^b) - a(\phi_h^* + g_h, \mathcal{P}_h \psi^b)}{\|b\|_{(H^{-s})'}} \right] . \end{aligned} \tag{30}$$

From Lemma 2.3 it follows that $\left\|\psi^b\right\|_{H^s} \sim \|b\|_{(H^{-s})'}$. Using Lemma 4.1 and the approximation property of $\mathcal{P}_h$ the first term can be estimated by

$$\begin{aligned} \frac{a(\phi + g - \phi_h^* - g_h, \psi^b - \mathcal{P}_h \psi^b)}{\|b\|_{(H^{-s})'}} &\lesssim \|\phi + g - \phi_h^* - g_h\|_{H^0} \frac{\left\|\psi^b - \mathcal{P}_h \psi^b\right\|_{H^0}}{\|\psi^b\|_{H^s}} \\ &\lesssim \left(h_x^r + h_t^{\frac{r}{2}} \right) \left(h_x^s + h_t^{\frac{s}{2}} \right) \|\phi + g\|_{H^r} . \end{aligned}$$

The second term in (30) can be estimated using (27), the inverse estimate, the stability of $\mathcal{P}_h$ and Lemma 4.2

$$\begin{aligned} \frac{a_h(\phi_h^* + g_h, \mathcal{P}_h \psi^b) - a(\phi_h^* + g_h, \mathcal{P}_h \psi^b)}{\|b\|_{(H^{-s})'}} &\lesssim \varepsilon_h \|\phi_h^* + g_h\|_{\check{H}} \frac{\left\|\mathcal{P}_h \psi^b\right\|_{\check{H}}}{\|\psi^b\|_{H^s}} \\ &\lesssim \varepsilon_h C^{\frac{1}{2}}(h) \|\phi + g\|_{H^{\frac{1}{2}}} \left(h_x^{-\frac{1}{2}+s} + h_t^{-\frac{1}{4}+\frac{s}{2}} \right) \frac{\left\|\mathcal{P}_h \psi^b\right\|_{H^s}}{\|\psi^b\|_{H^s}} . \end{aligned}$$

The assertion follows by combining (28) with the last two estimates. □

5 Conditioning of the Linear Systems

After the optimal realization of the discrete boundary integral operators via pFMM it remains to investigate the conditioning of the system matrices in the linear systems (22) and (23). Note that

the matrices V_0, $\mathsf{D}_{\kappa,0}$ and S_0 are symmetric positive definite, thus it suffices to derive bounds for the spectral condition number to predict the behavior of an iterative solver.

We denote by $\mathcal{V}_0$ the integral operator with the time integrated kernel $V_{h_t,0}$ given by (20). Furthermore, $\mathcal{D}_0$ is defined similarly for the hypersingular operator.

For estimates of the conditioning of V_0 and D_0 we consider functions in the ansatz space

$$q_h(\mathbf{x},t) = \phi_{h_t,0}(t)p_{h_x}(\mathbf{x}) \;, \quad \text{and} \quad u_h(\mathbf{x},t) = \phi_{h_t,0}(t)v_{h_x}(\mathbf{x}) \;, \tag{31}$$

where

$$p_{h_x}(\mathbf{x}) = \sum_k \varphi_{h_x,k}(\mathbf{x})p_k \;, \quad \text{and} \quad v_{h_x}(\mathbf{x}) = \sum_k \varphi_{h_x,k}(\mathbf{x})v_k \;. \tag{32}$$

The equivalences

$$\|p_{h_x}\|^2_{L_2(\Gamma)} \sim h_x^2 \,\|\mathsf{p}\|_2^2 \quad \text{and} \quad \|v_{h_x}\|^2_{L_2(\Gamma)} \sim h_x^2 \,\|\mathsf{v}\|_2^2 \;, \tag{33}$$

of the $L_2(\Gamma\times\Upsilon)$-norm of the function and the Euclidean norm of the coefficient vectors follow from the assumptions of the mesh refinement, see, e.g., [12]. By Theorem 2.3,

$$\big\langle \mathcal{V}_0 p_{h_x}, p_{h_x}\big\rangle_\Gamma = \big\langle \mathcal{V} q_h, q_h\big\rangle_{\Gamma\times\Upsilon} \sim \|q_h\|^2_{H^{-\frac{1}{2},-\frac{1}{4}}(\Gamma\times\Upsilon)} \;, \tag{34}$$

$$\langle \mathcal{D}_0 v_{h_x}, v_{h_x}\rangle_\Gamma = \langle \mathcal{D} u_h, u_h\rangle_{\Gamma\times\Upsilon} \sim \|u_h\|^2_{H^{\frac{1}{2},\frac{1}{4}}(\Gamma\times\Upsilon)} \;. \tag{35}$$

We begin with an estimate of $\phi_{h_t,0}$.

Lemma 5.1. *For $s \in \big(-\frac{1}{2},\frac{1}{2}\big)$ and $h_t \to 0$ the estimate*

$$\|\phi_{h_t,0}\|_{H^s(\mathbb{R})} \sim h_t^{\frac{1}{2}-s}$$

holds.

Proof. Because of the scaling $\phi_{h_t,0}(t) = \phi_{loc}(t/h_t)$ it follows that the Fourier transform $\hat\phi_{h_t}$ of ϕ_{h_t} satisfies $\hat\phi_{h_t}(\tau) = h_t\hat\phi_{loc}(h_t\tau)$. Thus the change of variables $\rho = h_t\tau$ gives

$$\|\phi_{h_t}\|^2_{H^s(\mathbb{R})} = h_t^2 \int_{\mathbb{R}} (1+\tau^2)^s \left|\hat\phi_{loc}(h_t\tau)\right|^2 \mathrm{d}\tau = h_t^{1-2s} \int_{\mathbb{R}} (h_t^2+\rho^2)^s \left|\hat\phi_{loc}(\rho)\right|^2 \mathrm{d}\rho \;. \tag{36}$$

It remains to verify that the last integral can be bounded from above and below independently of h_t. To that end, consider the case $s \geq 0$ first. A lower bound can be obtained by dropping the factor h_t in the integrand of (36). Thus

$$\|\phi_{h_t}\|^2_{H^s(\mathbb{R})} \geq {h_t}^{1-2s} \int_{\mathbb{R}} \rho^{2s} \left|\hat\phi_{loc}(\rho)\right|^2 \mathrm{d}\rho \;, \qquad s \geq 0 \;.$$

Since the latter integral is positive, the first part of the assertion is verified. An upper bound can be obtained by replacing h_t in the integrand of (36) with unity, thus

$$\|\phi_{h_t}\|^2_{H^s(\mathbb{R})} \leq h_t^{1-2s} \int_{\mathbb{R}} (1+\rho^2)^s \left|\hat\phi_{loc}(\rho)\right|^2 \mathrm{d}\rho \;, \qquad s \geq 0 \;.$$

Since $\|\phi_{loc}\|_{H^s(\mathbb{R})}$ is finite this establishes the next part of the assertion. The argument for negative s is the same, with the exception that dropping h_t in (36) will give the upper bound and replacing h_t by unity will give the lower bound of $\|\phi_{h_t}\|_{H^s(\mathbb{R})}$. □

Lemma 5.2. *For $h_t \to 0$ the function $u_h(\mathbf{x},t)$ defined in* (31) *satisfies*

$$\|u_h\|^2_{H^{\frac{1}{2},\frac{1}{4}}(\Gamma\times\Upsilon)} \sim h_t \|v_{h_x}\|^2_{H^{\frac{1}{2}}(\Gamma)} + h_t^{\frac{1}{2}} \|v_{h_x}\|^2_{L_2(\Gamma)} .$$

Proof. The Fourier transform of $u_h(\mathbf{x},t)$ in time is $\hat{u}_h(\mathbf{x},\tau) = v_{h_x}(\mathbf{x})\hat{\phi}_{h_t}(\tau)$. Moreover, the definition of the $H^{\frac{1}{2},\frac{1}{4}}(\Gamma\times\mathbb{R})$ norm in (9) implies that

$$\begin{aligned}\|u_h\|^2_{H^{\frac{1}{2},\frac{1}{4}}(\Gamma\times\mathbb{R})} &= \int_{\mathbb{R}} \|\hat{u}_h(\cdot,\tau)\|^2_{H^{\frac{1}{2}}(\Gamma)} + \left(1+\tau^2\right)^{\frac{1}{4}} \|\hat{u}_h(\cdot,\tau)\|^2_{L_2(\Gamma)}\,\mathrm{d}\tau \\ &= \|\phi_{h_t}\|^2_{L_2(\mathbb{R})} \|v_{h_x}\|^2_{H^{\frac{1}{2}}(\Gamma)} + \|\phi_{h_t}\|^2_{H^{\frac{1}{4}}(\mathbb{R})} \|v_{h_x}\|^2_{L_2(\Gamma)} .\end{aligned}$$

Thus the assertion follows from Lemma 5.1 and the fact that $\|u_h\|_{H^{\frac{1}{2},\frac{1}{4}}(\Gamma\times\mathbb{R})} = \|u_h\|_{H^{\frac{1}{2},\frac{1}{4}}(\Gamma\times\Upsilon)}$. □

Lemma 5.3. *For $h_t \to 0$ the function $q_h(\mathbf{x},t)$ defined in* (31) *satisfies*

$$\|q_h\|^2_{H^{-\frac{1}{2},-\frac{1}{4}}(\Gamma\times\Upsilon)} \lesssim h_t^{\frac{3}{2}} \|p_{h_x}\|^2_{L_2(\Gamma)} .$$

Proof. The negative norm is defined by the duality

$$\begin{aligned}\|q_h\|_{H^{-\frac{1}{2},-\frac{1}{4}}(\Gamma\times\Upsilon)} &= \sup_{0\neq\varphi\in H^{\frac{1}{2},\frac{1}{4}}(\Gamma\times\Upsilon)} \frac{\langle q_h,\varphi\rangle_{\Gamma\times\Upsilon}}{\|\varphi\|_{H^{\frac{1}{2},\frac{1}{4}}(\Gamma\times\Upsilon)}} \\ &= \sup_{0\neq\varphi\in H^{\frac{1}{2},\frac{1}{4}}(\Gamma\times\mathbb{R})} \frac{\langle q_h,\varphi\rangle_{\Gamma\times\mathbb{R}}}{\|\varphi\|_{H^{\frac{1}{2},\frac{1}{4}}(\Gamma\times\mathbb{R})}} . \qquad (37)\end{aligned}$$

Here the duality pairing is given by

$$\langle q_h,\varphi\rangle_{\Gamma\times\mathbb{R}} = \int_{\mathbb{R}}\int_{\Gamma} \phi_{h_t}(t)p_{h_x}(\mathbf{x})\varphi(\mathbf{x},t)\mathrm{d}s_{\mathbf{x}}\mathrm{d}t = \int_{\mathbb{R}}\int_{\Gamma} \hat{\phi}_{h_t}(\tau)p_{h_x}(\mathbf{x})\hat{\varphi}(\mathbf{x},\tau)\mathrm{d}s_{\mathbf{x}}\mathrm{d}\tau .$$

where the second step is Parseval's identity. We estimate this integral using the Cauchy-Schwarz inequality for the Γ-integral and the duality in the $H^{-\frac{1}{4}}(\Upsilon)$ norm for the τ-integral. That is,

$$\begin{aligned}\left|\langle q_h,\varphi\rangle_{\Gamma\times\mathbb{R}}\right|^2 &\le \|p_{h_x}\|^2_{L_2(\Gamma)} \int_{\mathbb{R}} \left(1+\tau^2\right)^{-\frac{1}{4}} \left|\hat{\phi}_{h_t}(\tau)\right|^2 \mathrm{d}\tau \int_{\mathbb{R}} \left(1+\tau^2\right)^{\frac{1}{4}} \|\hat{\varphi}(\cdot,\tau)\|^2_{L_2(\Gamma)}\,\mathrm{d}\tau \\ &\le \|p_{h_x}\|^2_{L_2(\Gamma)} \|\phi_{h_t}\|^2_{H^{-\frac{1}{4}}(\Upsilon)} \|\varphi\|^2_{H^{\frac{1}{2},\frac{1}{4}}(\Gamma\times\mathbb{R})}\end{aligned}$$

and the assertion follows from (37) and Lemma 5.1. □

Theorem 5.1. *For $h_t \to 0$ the eigenvalues and spectral condition numbers of V_0 and D_0 satisfy the bounds*

$$\lambda_{max}(\mathsf{V}_0) \lesssim h_t^{\frac{3}{2}} h_x^2 , \qquad \lambda_{max}(\mathsf{D}_0) \lesssim \left(h_x^{-\frac{1}{2}} + h_t^{-\frac{1}{4}} \right)^2 h_x^2 h_t ,$$

$$\lambda_{min}(\mathsf{V}_0) \gtrsim \left(h_x^{-\frac{1}{2}} + h_t^{-\frac{1}{4}} \right)^{-2} h_x^2 h_t , \qquad \lambda_{min}(\mathsf{D}_0) \gtrsim h_x^2 h_t^{\frac{1}{2}} ,$$

$$cond(\mathsf{V}_0) \lesssim 1 + \left(\frac{h_t}{h_x^2} \right)^{\frac{1}{2}} , \qquad cond(\mathsf{D}_0) \lesssim 1 + \left(\frac{h_t}{h_x^2} \right)^{\frac{1}{2}} .$$

Proof. Let q_h, p_{h_x} and p be defined by (31) and (32). From (34), Theorem 3.2, (33) and Lemma 5.1 we have

$$\begin{aligned} \lambda_{\min}(\mathsf{V}_0) &= \min_{\mathsf{p}\neq 0} \frac{\mathsf{p}^\top \mathsf{V}_0 \mathsf{p}}{\|\mathsf{p}\|_2^2} = \min_{\mathsf{p}\neq 0} \frac{\langle \mathcal{V}_0 p_{h_x}, p_{h_x} \rangle_\Gamma}{\|\mathsf{p}\|_2^2} \gtrsim \min_{\mathsf{p}\neq 0} \frac{\|q_h\|^2_{H^{-\frac{1}{2},-\frac{1}{4}}(\Gamma\times\Upsilon)}}{\|\mathsf{p}\|_2^2} \\ &\gtrsim \left(h_x^{-\frac{1}{2}} + h_t^{-\frac{1}{4}} \right)^{-2} \min_{\mathsf{p}\neq 0} \frac{\|p_{h_x}\|^2_{L_2(\Gamma)} \|\phi_{h_t}\|^2_{L_2(\Upsilon)}}{\|\mathsf{p}\|_2^2} \gtrsim \left(h_x^{-\frac{1}{2}} + h_t^{-\frac{1}{4}} \right)^{-2} h_x^2 h_t . \end{aligned}$$

Likewise, from Lemma 5.3 we get

$$\lambda_{\max}(\mathsf{V}_0) = \max_{\mathsf{p}\neq 0} \frac{\mathsf{p}^\top \mathsf{V}_0 \mathsf{p}}{\|\mathsf{p}\|_2^2} \lesssim \max_{\mathsf{p}\neq 0} \frac{\|q_h\|^2_{H^{-\frac{1}{2},-\frac{1}{4}}(\Gamma\times\Upsilon)}}{\|\mathsf{p}\|_2^2} \lesssim h_t^{\frac{3}{2}} \max_{\mathsf{p}\neq 0} \frac{\|p_{h_x}\|^2_{L_2(\Gamma)}}{\|\mathsf{p}\|_2^2} \lesssim h_t^{\frac{3}{2}} h_x^2 .$$

To estimate the eigenvalues of D_0 we consider u_h, v_{h_x} and v as defined in (31) and (32). From (35), Lemma 5.2 and the norm equivalence (5.2) we get

$$\lambda_{\min}(\mathsf{D}_0) = \min_{\mathsf{v}\neq 0} \frac{\mathsf{v}^\top \mathsf{D}_0 \mathsf{v}}{\|\mathsf{v}\|_2^2} \gtrsim \min_{\mathsf{v}\neq 0} \frac{\|u_h\|^2_{H^{\frac{1}{2},\frac{1}{4}}(\Gamma\times\Upsilon)}}{\|\mathsf{v}\|_2^2} \gtrsim h_t^{\frac{1}{2}} \min_{\mathsf{v}\neq 0} \frac{\|v_{h_x}\|^2_{L_2(\Gamma)}}{\|\mathsf{v}\|_2^2} \gtrsim h_t^{\frac{1}{2}} h_x^2 .$$

Moreover, from Theorem 3.2 it follows that

$$\begin{aligned} \lambda_{\max}(\mathsf{D}_0) &= \max_{\mathsf{v}\neq 0} \frac{\mathsf{v}^\top \mathsf{D}_0 \mathsf{v}}{\|\mathsf{v}\|_2^2} \lesssim \max_{\mathsf{v}\neq 0} \frac{\|u_h\|^2_{H^{\frac{1}{2},\frac{1}{4}}(\Gamma\times\Upsilon)}}{\|\mathsf{v}\|_2^2} \\ &\lesssim \left(h_x^{-\frac{1}{2}} + h_t^{-\frac{1}{4}} \right)^2 \max_{\mathsf{v}\neq 0} \frac{\|v_{h_x}\|^2_{L_2(\Gamma)} \|\phi_{h_t}\|^2_{L_2(\Upsilon)}}{\|\mathsf{v}\|_2^2} \lesssim \left(h_x^{-\frac{1}{2}} + h_t^{-\frac{1}{4}} \right)^2 h_x^2 h_t . \end{aligned}$$

The condition numbers are finally derived by taking the ratios of the estimates for the extremal eigenvalues. □

We now turn to the discrete Dirichlet to Robin operator in (24).

Theorem 5.2. *For $h_t \to 0$ the eigenvalues and spectral condition numbers of S_0 satisfy the bounds*

$$\begin{aligned}
&\lambda_{min}(\mathsf{S}_0) \gtrsim h_t^{\frac{1}{2}} h_x^2 \,, \\
&\lambda_{max}(\mathsf{S}_0) \lesssim \left(1 + \left(\frac{h_t}{h_x^2}\right)^{\frac{1}{4}}\right) \left(h_x^{-\frac{1}{2}} + h_t^{-\frac{1}{4}}\right)^2 h_x^2 h_t \,, \\
&cond(\mathsf{S}_0) \lesssim 1 + \left(\frac{h_t}{h_x^2}\right)^{\frac{3}{4}} .
\end{aligned}$$

Proof. Let v_{h_x}, p_{h_x}, u_h and q_h be defined as in (31). Further, in view of (24), we define the vector

$$\mathsf{c} = \left(\frac{1}{2}\mathsf{M} + \mathsf{K}_0\right)\mathsf{v}$$

then

$$\mathsf{v}^\top \mathsf{S}_0 \mathsf{v} = \mathsf{v}^\top \mathsf{D}_{\kappa,0} \mathsf{v} + \mathsf{c}^\top \mathsf{V}_0^{-1} \mathsf{c}. \tag{38}$$

Since V_0^{-1} is symmetric positive definite and since $\kappa \geq 0$ it follows that

$$\mathsf{v}^\top \mathsf{S}_0 \mathsf{v} \geq \lambda_{\min}(\mathsf{D}_0) \, \|\mathsf{v}\|_2^2$$

which implies the first assertion.

For the second assertion, we estimate, using Lemma 5.3 and the inverse estimate

$$\begin{aligned}
\|\mathsf{c}\|_2 = \sup_{\mathsf{p}\neq 0} \frac{\mathsf{p}^\top \mathsf{c}}{\|\mathsf{p}\|_2} \;&=\; \sup_{\mathsf{p}\neq 0} \frac{\left\langle \left(\frac{1}{2} + \mathcal{K}\right) u_h, q_h \right\rangle_{\Gamma\times\Upsilon}}{\|\mathsf{p}\|_2} \\
&\lesssim \sup_{\mathsf{p}\neq 0} \frac{\|u_h\|_{H^{\frac{1}{2},\frac{1}{4}}(\Gamma\times\Upsilon)} \, \|q_h\|_{H^{-\frac{1}{2},-\frac{1}{4}}(\Gamma\times\Upsilon)}}{\|\mathsf{p}\|_2} \\
&\lesssim \left(h_x^{-\frac{1}{2}} + h_t^{-\frac{1}{4}}\right) h_t^{\frac{3}{4}} \sup_{\mathsf{p}\neq 0} \frac{\|u_h\|_{L_2(\Gamma\times\Upsilon)} \, \|p_{h_x}\|_{L_2(\Gamma)}}{\|\mathsf{p}\|_2} \\
&\lesssim \left(h_x^{-\frac{1}{2}} + h_t^{-\frac{1}{4}}\right) h_t^{\frac{5}{4}} h_x^2 \, \|\mathsf{v}\|_2
\end{aligned}$$

Thus it follows from (38) and Theorem 5.1 that

$$\begin{aligned}
\mathsf{v}^\top \mathsf{S}_0 \mathsf{v} &\leq \lambda_{\max}(\mathsf{D}_{\kappa,0}) \, \|\mathsf{v}\|_2^2 + \lambda_{\min}^{-1}(\mathsf{V}_0) \, \|\mathsf{c}\|_2^2 \\
&\lesssim \left(1 + \left(\frac{h_t}{h_x^2}\right)^{\frac{1}{4}}\right) \left(h_x^{-\frac{1}{2}} + h_t^{-\frac{1}{4}}\right) h_t h_x^2 \, \|\mathsf{v}\|_2^2
\end{aligned}$$

which implies the second and third assertion. □

Our main result is a simple consequence of the previous estimates.

Corollary 5.1. *If $h_t \lesssim h_x^2$ then the spectral condition number of $\mathsf{V}_0, \mathsf{D}_0$ and S_0 is independent of the meshwidth.*

6 Numerical Examples

6.1 Condition of V_0 and D_0

In this section we experimentally investigate the eigenvalues and spectral condition number of V_0 and D_0. We choose our domain to be the unit cube, i.e., $\Omega = (-0.5, 0.5)^3$, times the unit time interval $\Upsilon = (0, 1)$. The coarsest discretization consists of four equally sized triangles on each face of the unit cube times one unit timestep. Starting from this discretization we perform four uniform spatial and eight uniform temporal refinements.

Table 1 through 3 display the extremal eigenvalues and spectral condtion number of V_0, normalized by the estimates given by Theorem 5.1. One should expect that these ratios stay bounded away from zero and infinity, and it appears that they indeed do, at least in the lower right corners of the tables. Table 4 through 6 display the analogous data for D_0.

	$h_x = 2^{\,0}$	$h_x = 2^{-1}$	$h_x = 2^{-2}$	$h_x = 2^{-3}$	$h_x = 2^{-4}$
$h_t = 2^{\,0}$	0.0914	0.0916	0.0918	0.0922	0.0919
$h_t = 2^{-1}$	0.1004	0.1006	0.1009	0.1008	0.1006
$h_t = 2^{-2}$	0.1040	0.1040	0.1043	0.1044	0.1044
$h_t = 2^{-3}$	0.1034	0.1041	0.1039	0.1040	0.1043
$h_t = 2^{-4}$	0.1024	0.1021	0.1023	0.1024	0.1022
$h_t = 2^{-5}$	0.1005	0.1006	0.1008	0.1008	0.1006
$h_t = 2^{-6}$	0.0988	0.0991	0.0991	0.0996	0.0996
$h_t = 2^{-7}$	0.0976	0.0979	0.0982	0.0992	0.0990
$h_t = 2^{-8}$	0.0967	0.0970	0.0976	0.0980	0.0985

Table 1: $\lambda_{max}(\mathsf{V}_0)/\left[h_x^2 h_t^{\frac{3}{2}}\right]$

	$h_x = 2^{\,0}$	$h_x = 2^{-1}$	$h_x = 2^{-2}$	$h_x = 2^{-3}$	$h_x = 2^{-4}$
$h_t = 2^{\,0}$	0.0326	0.0249	0.0196	0.0160	0.0136
$h_t = 2^{-1}$	0.0389	0.0289	0.0221	0.0176	0.0148
$h_t = 2^{-2}$	0.0469	0.0340	0.0253	0.0196	0.0160
$h_t = 2^{-3}$	0.0571	0.0405	0.0295	0.0222	0.0177
$h_t = 2^{-4}$	0.0693	0.0490	0.0347	0.0253	0.0196
$h_t = 2^{-5}$	0.0825	0.0595	0.0413	0.0295	0.0222
$h_t = 2^{-6}$	0.0947	0.0719	0.0499	0.0347	0.0254
$h_t = 2^{-7}$	0.1041	0.0854	0.0607	0.0415	0.0295
$h_t = 2^{-8}$	0.1094	0.0976	0.0731	0.0500	0.0348

Table 2: $\lambda_{min}(\mathsf{V}_0)/\left[\left(h_x^{-\frac{1}{2}} + h_t^{-\frac{1}{4}}\right)^{-2} h_x^2 h_t\right]$

	$h_x = 2^{\,0}$	$h_x = 2^{-1}$	$h_x = 2^{-2}$	$h_x = 2^{-3}$	$h_x = 2^{-4}$
$h_t = 2^{\,0}$	5.6074	7.1340	8.4412	9.3567	9.9144
$h_t = 2^{-1}$	5.1220	6.9087	8.5786	9.8093	10.5497
$h_t = 2^{-2}$	4.3118	6.1090	8.0138	9.5775	10.6316
$h_t = 2^{-3}$	3.4035	5.1034	6.9929	8.8049	10.1273
$h_t = 2^{-4}$	2.6611	4.0487	5.9043	7.8616	9.3835
$h_t = 2^{-5}$	2.0868	3.1793	4.8421	6.7738	8.4979
$h_t = 2^{-6}$	1.6986	2.4821	3.8596	5.7358	7.6076
$h_t = 2^{-7}$	1.4503	1.9646	3.0413	4.7484	6.6624
$h_t = 2^{-8}$	1.2989	1.6191	2.4032	3.8066	5.6634

Table 3: $\mathrm{cond}(\mathsf{V}_0)/\left[1+(h_t/h_x^2)^{\frac{1}{2}}\right]$

	$h_x = 2^{\,1}$	$h_x = 2^{\,0}$	$h_x = 2^{-1}$	$h_x = 2^{-2}$	$h_x = 2^{-3}$
$h_t = 2^{\,0}$	0.1003	0.1757	0.2347	0.2930	0.3461
$h_t = 2^{-1}$	0.0860	0.1534	0.2080	0.2664	0.3213
$h_t = 2^{-2}$	0.0748	0.1350	0.1823	0.2389	0.2955
$h_t = 2^{-3}$	0.0660	0.1202	0.1586	0.2124	0.2683
$h_t = 2^{-4}$	0.0820	0.1115	0.1389	0.1862	0.2412
$h_t = 2^{-5}$	0.0995	0.1148	0.1242	0.1624	0.2134
$h_t = 2^{-6}$	0.1170	0.1276	0.1212	0.1408	0.1880
$h_t = 2^{-7}$	0.1331	0.1429	0.1274	0.1254	0.1638
$h_t = 2^{-8}$	0.1485	0.1589	0.1399	0.1233	0.1423

Table 4: $\lambda_{max}(\mathsf{D}_0)/\left[\left(h_x^{-\frac{1}{2}}+h_t^{-\frac{1}{4}}\right)^2 h_x^2 h_t\right]$

	$h_x = 2^{\,1}$	$h_x = 2^{\,0}$	$h_x = 2^{-1}$	$h_x = 2^{-2}$	$h_x = 2^{-3}$
$h_t = 2^{\,0}$	0.0697	0.0776	0.0802	0.0813	0.0814
$h_t = 2^{-1}$	0.0950	0.1047	0.1091	0.1104	0.1111
$h_t = 2^{-2}$	0.1134	0.1336	0.1414	0.1446	0.1454
$h_t = 2^{-3}$	0.0874	0.1527	0.1688	0.1749	0.1774
$h_t = 2^{-4}$	0.0720	0.1414	0.1811	0.1943	0.1987
$h_t = 2^{-5}$	0.0645	0.1122	0.1747	0.2009	0.2100
$h_t = 2^{-6}$	0.0614	0.0918	0.1498	0.1951	0.2130
$h_t = 2^{-7}$	0.0553	0.0765	0.1202	0.1774	0.2077
$h_t = 2^{-8}$	0.0525	0.0659	0.0970	0.1505	0.1962

Table 5: $\lambda_{min}(\mathsf{D}_0)/\left[h_x^2 h_t^{\frac{1}{2}}\right]$

	$h_x = 2^{\,1}$	$h_x = 2^{\,0}$	$h_x = 2^{-1}$	$h_x = 2^{-2}$	$h_x = 2^{-3}$
$h_t = 2^{\,0}$	2.8766	4.3986	5.2695	5.8705	6.2523
$h_t = 2^{-1}$	1.7957	2.9107	3.5821	4.1372	4.4705
$h_t = 2^{-2}$	1.2816	2.0210	2.5038	2.9735	3.3099
$h_t = 2^{-3}$	1.4178	1.5621	1.8656	2.2822	2.5936
$h_t = 2^{-4}$	2.0489	1.5309	1.5336	1.8621	2.1856
$h_t = 2^{-5}$	2.6462	1.9215	1.4114	1.6046	1.9095
$h_t = 2^{-6}$	3.1059	2.5003	1.5726	1.4436	1.7147
$h_t = 2^{-7}$	3.7203	3.2030	1.9916	1.4035	1.5656
$h_t = 2^{-8}$	4.1607	3.9266	2.5963	1.5918	1.4509

Table 6: $\mathrm{cond}(\mathsf{D}_0)/\left[1+(h_t/h_x^2)^{\frac{1}{2}}\right]$

6.2 Initial Boundary Value Problems

In this section we solve homogeneous initial boundary value problems described in Section 2 for $\Omega = (-0.5, 0.5)^3$ and $\Upsilon = (0, 0.5)$. In all cases, we choose the boundary data corresponding to a heat point source $g_D(\mathbf{x},t) = G(\mathbf{x}-\mathbf{x}_0,t)$, $g_N(\mathbf{x},t) = \partial_{n_\mathbf{x}} G(\mathbf{x}-\mathbf{x}_0,t)$, and $g_R(\mathbf{x},t) = \partial_{n_\mathbf{x}} G(\mathbf{x}-\mathbf{x}_0,t) + \kappa(\mathbf{x})G(\mathbf{x}-\mathbf{x}_0,t)$ located at $\mathbf{x}_0 := (1.5, 1.5, 1.5)^\top$ with $\kappa = 1$.

We monitor errors of q and u in the $L_2(\Gamma\times\Upsilon)$-norm. Setting $r = \frac{3}{2}$ and $s = \frac{1}{2}$ in Lemma 4.2 shows that the optimal theoretical convergence rate for q is $O(h_x + \sqrt{h_t})$. If the endpoint $s = \frac{1}{2}$ was included in the assumption of Lemma 4.3, the optimal convergence rate of u would be $O\left(h_x^2 + h_t\right)$. However, the endpoint cannot be reached because it is not known whether the statement of Theorem 2.3 can be extended to $s = \frac{1}{2}$, see [4]. However, our numerical result reproduces this optimal result, at least for the geometry considered.

6.2.1 Initial Dirichlet BVP

In our first example we solve the pFMM approximated variational form related to the initial Dirichlet boundary value problem (16). In Table 7 we present errors, iteration numbers, computation time and memory requirement for a $h_t = O(h_x^2)$ refinement scheme. We observe that the optimal $h_x + \sqrt{h_t}$ convergence is achieved. Furthermore, the solution is obtained in optimal complexity with respect to the total number of unknowns $N_x N_t$, thanks to the application of the pFMM and the bounded number of iterations $\#\mathsf{V}_0$ implied by Theorem 5.1.

$N_x N_t$	$\left\|q - q_h^*\right\|_{L_2} / \left\|q\right\|_{L_2}$	$\#\mathsf{V}_0$	cpu[sec]	mem[GB]
12,288	1.23 10^{-1}	10	4.54 10^{1}	5.68 10^{-2}
196,608	6.07 10^{-2}	10	1.83 10^{2}	2.05 10^{-1}
3,145,728	3.01 10^{-2}	10	3.35 10^{3}	1.07 $10^{\,0}$
50,331,648	1.50 10^{-2}	10	1.12 10^{5}	6.29 $10^{\,0}$

Table 7: Dirichlet IBVP with uniform $h_t = O(h_x^2)$ refinement.

6.2.2 Initial Neumann BVP

We solve the pFMM approximated variational form related to the initial Neumann boundary value problem (17). In Table 8 we present results for a $h_t = O(h_x^2)$ refinement, which reveals that the $O(h_t)$ behavior of the space-time Galerkin scheme is obtained in optimal complexity, again thanks to pFMM algorithm and the bounded number of iterations $\#\mathsf{D}_0$.

$N_x N_t$	$\left\|u-u_h^*\right\|_{L_2} / \left\|u\right\|_{L_2}$	$\#\mathsf{D}_0$	cpu[sec]	mem[GB]
6,208	$2.76\ 10^{-2}$	8	$1.04\ 10^{2}$	$4.55\ 10^{-2}$
98,560	$6.65\ 10^{-3}$	8	$3.37\ 10^{2}$	$2.09\ 10^{-1}$
1,573,888	$1.65\ 10^{-3}$	8	$4.93\ 10^{3}$	$1.09\ 10^{0}$
25,169,920	$4.10\ 10^{-4}$	8	$1.55\ 10^{5}$	$6.88\ 10^{0}$

Table 8: Neumann IBVP with uniform $h_t = O(h_x^2)$ refinement.

6.2.3 Initial Robin BVP

We solve the pFMM approximated variational form related to the initial Robin boundary value problem (18). In Table 9 we present more details for a $h_t = O(h_x^2)$ refinement scheme. Again, they reveal the $O(h_t)$ behavior of the nearly optimal computational complexity.

$N_x N_t$	$\left\|u-u_h^*\right\|_{L_2} / \left\|u\right\|_{L_2}$	$\#\mathsf{S}_0^*$	cpu[sec]	mem[GB]
6,208	$2.19\ 10^{-2}$	10	$1.43\ 10^{2}$	$8.85\ 10^{-2}$
98,560	$5.46\ 10^{-3}$	10	$4.96\ 10^{2}$	$3.55\ 10^{-1}$
1,573,888	$1.36\ 10^{-3}$	10	$8.16\ 10^{3}$	$2.00\ 10^{0}$
25,169,920	$3.41\ 10^{-4}$	9	$2.58\ 10^{5}$	$1.12\ 10^{1}$

Table 9: Robin IBVP with uniform $h_t = O(h_x^2)$ refinement.

6.2.4 Mixed Initial BVP

Finally, we solve the pFMM approximated variational form of the mixed initial boundary value problem (1). For our example below we have choosen $\Gamma_D = (-0.5,0.5) \times -0.5 \times (-0.5,0.5)$, $\Gamma_N = (-0.5,0.5) \times 0.5 \times (-0.5,0.5)$, and $\overline{\Gamma}_R = \Gamma \setminus (\overline{\Gamma}_N \cup \overline{\Gamma}_D)$. The data in Table Table 10 display the same convergence and complexity behavior of the algorithm as the other problems.

$N_x N_t$	$\left\|u-u_h^*\right\|_{L_2} / \left\|u\right\|_{L_2}$	$\#\mathsf{S}_0^*$	cpu[sec]	mem[GB]
6,208	$2.19\ 10^{-2}$	10	$1.52\ 10^{2}$	$7.46\ 10^{-2}$
98,560	$5.45\ 10^{-2}$	10	$5.64\ 10^{2}$	$3.54\ 10^{-1}$
1,573,888	$1.36\ 10^{-3}$	10	$9.62\ 10^{3}$	$1.94\ 10^{0}$
25,169,920	$3.41\ 10^{-4}$	9	$2.80\ 10^{5}$	$1.19\ 10^{1}$

Table 10: Mixed IBVP with uniform $h_t = O(h_x^2)$ refinement.

6.3 Industrial Application

Our method has been used for the thermal simulation of hot forming tools in joint work with W. Weiss, who developed the thermal model in his PhD thesis [15]. The idea of using boundary element methods is motivated by the fact that the geometry of hot forming tools is extremely complicated (especially the cooling chanel geometry inside the tools) and only the surface temperature of the tool is required.

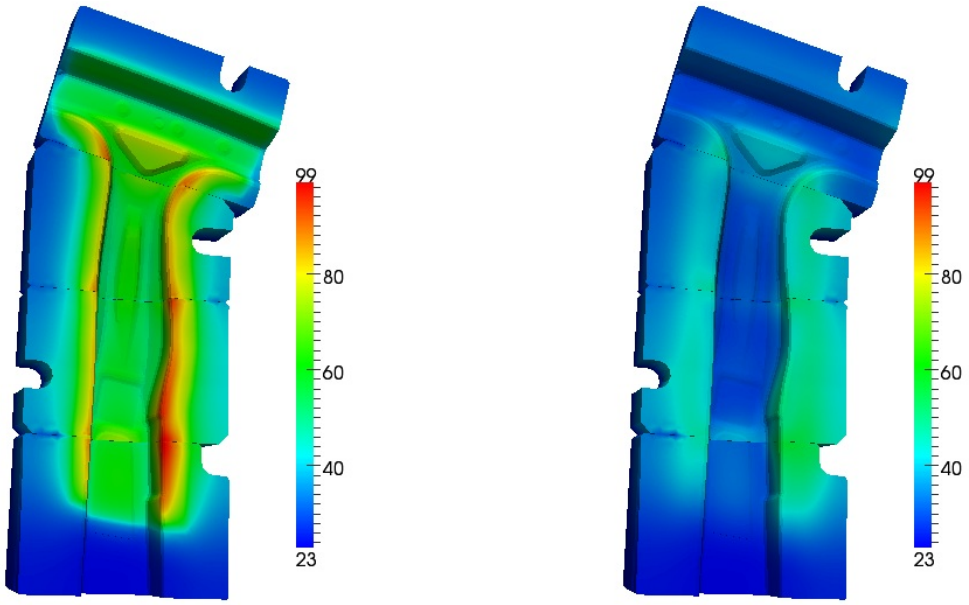

(a) Quasi-static working temperature [°C].

(b) Closing temperature [°C].

Figure 1: Significant temperatures of the hot forming tool.

The hot forming process consists of two main steps: Fast forming and rapid cooling of the blank in the closed and cooled tool. The model in [15] consists of an energetic averaging of the individual cycles until the *quasi-static working temperature* is reached followed by one cooling cycle in order to compute the *closing temperature* of the tools before the next hot blank is formed. This model leads to the mixed Dirichlet-Robin IBVP (14), which can be transformed trivially to have zero temperature Dirichlet boundary conditions, and homogeneous initial conditions.

Figure 1 shows the *quasi-static working temperature* and the *closing temperature* of the tool (the whole setup consists of an upper and a lower tool, however only the results for the upper tool are shown). These numerical simulations have been verified experimentally by measurements during the real process. On several significant points inside the tools thermo-elements have been installed with one exemplary comparison shown in Figure 2. Observe, that [15]'s model is based on an energetic averaging of the real process, thus the simulation can not reproduce the individual cycles.

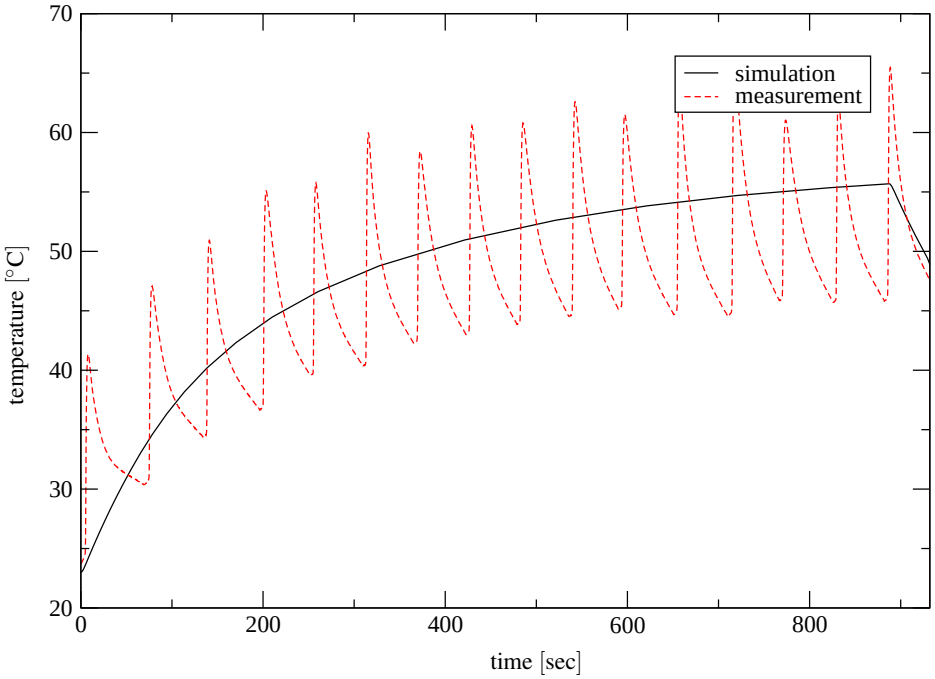

Figure 2: Temperature comparison – simulation vs. measurement [15].

Acknowledgments

The work of Michael Messner was supported by the *Austrian Marshall-Plan Foundation*, while the work of Johannes Tausch is supported by the National Science Foundation under grant DMS-1115931.

References

[1] D. Arnold and P. J. Noon. Coercivity of the single layer heat potential. *J. Comput. Math.*, 7:100–104, 1989.

[2] Dietrich Braess. *Finite Elements*. Cambridge, 3rd edition, 2007.

[3] R. M. Brown. The method of layer potentials for the heat equation in Lipschitz cylinders. *Amer. J. Math.*, 111:339–379, 1989.

[4] M. Costabel. Boundary integral operators for the heat equation. *Integr. Eq. Oper. Theory*, 13:498–552, 1990.

[5] L. Greengard and J. Strain. A fast algorithm for the evaluation of heat potentials. *Comm. Pure Appl. Math.*, XLIII:949–963, 1990.

[6] M. Messner. *A fast multipole Galerkin boundary element method for the transient heat equation*. PhD thesis, Graz University of Technology, 2014.

[7] M. Messner, J. Tausch, and M. Schanz. Fast Galerkin method for parabolic space-time boundary integral equations. *J. Comput. Phys.*, 258:15–30, 2014.

[8] N. Nishimura. Fast multipole accelerated boundary integral equation methods. *Appl. Mech. Rev.*, 55:299–323, 2002.

[9] P. J. Noon. *The single layer heat potential and Galerkin boundary element methods for the heat equation*. PhD thesis, University of Maryland, 1988.

[10] G. Of, O. Steinbach, and W. Wendland. The fast multipole method for the symmetric boundary integral formulation. *IMA J. Numer. Anal.*, 26:272–296, 2006.

[11] W. Pogorzelski, A. Kacner, J. Schorr-Con, and Z. S. Olesiak. *Integral equations and their applications*, volume 1. Pergamon Press Oxford, 1966.

[12] O. Steinbach. *Numerical approximation methods for elliptic boundary value problems*. Springer, 2008.

[13] J. Tausch. A fast method for solving the heat equation by layer potentials. *J. Comput. Phys.*, 224:956–969, 2007.

[14] J. Tausch. Fast Nyström methods for parabolic boundary integral equations. In U. Langer, M. Schanz, O. Steinbach, and W. L. Wendland, editors, *Fast Boundary Element Methods in Engineering and Industrial Applications*, volume 63 of *Lecture Notes in Applied and Computational Mechanics*, pages 185–219. Springer, 2011.

[15] W. Weiss. *Thermische Auslegung von Werkzeugen für Presshärteprozesse*. PhD thesis, Graz University of Technology, 2014.